International Journal of Nanomedicine

Dovepress
Taylor & Francis Group

Open Access Full Text Article

REVIEW

Research Progress on Nucleus-Targeting Carbon Nanoparticles for Tumor Imaging and Therapy

Hongkai Mu[1,*], Wenhui Dong[1,*], Lin Chen[2], Qiang Li[3], Boyang Xue[2], Yanjiao Xing[2], Jie Liu[1], Yingying Wei[4], Jiangbo Fan[5], TingTing Liang[6], Yongzhen Yang[2], Shiping Yu[4]

[1]Medical Imaging Department, Shanxi Medical University, Taiyuan, 030001, People's Republic of China; [2]Key Laboratory of Interface Science and Engineering in Advanced Materials, Ministry of Education, Taiyuan University of Technology, Taiyuan, 030024, People's Republic of China; [3]Interventional Therapy Department, Second Hospital of Shanxi Medical University, Taiyuan, 030032, People's Republic of China; [4]Interventional Therapy Department, Shanxi Province Cancer Hospital, Shanxi Hospital Affiliated to Cancer Hospital, Chinese Academy of Medical Sciences, Cancer Hospital Affiliated to Shanxi Medical University, Taiyuan, 030013, People's Republic of China; [5]Interventional Therapy Department, Shanxi Province People's Hospital, Taiyuan, 030000, People's Republic of China; [6]Obstetrics and Gynecology Department, Second Hospital of Shanxi Medical University, Taiyuan, 030032, People's Republic of China

*These authors contributed equally to this work

Correspondence: Yongzhen Yang; Shiping Yu, Email yangyongzhen@tyut.edu.cn; yushiping6@126.com

Abstract: The cell nucleus, as the central hub of cellular physiological activities, represents an effective target for cancer therapy. Targeting strategies aimed at the cell nucleus can enhance the delivery of more drugs into the tumor cell nucleus, thereby improving therapeutic efficacy. Such approaches can overcome the limitations of previous tissue- and cell-level treatments, such as insufficient specificity and excessive toxic side effects. Currently, researchers have integrated carbon nanoparticles (CNPs), therapeutic molecules, and nucleus-targeting components to construct various nucleus-targeted carbon nanoparticle delivery systems for tumor imaging and treatment. These systems not only increase drug concentration within the cell nucleus but also enable certain CNPs to utilize their intrinsic fluorescence for imaging monitoring. This review summarizes the latest classification progress of nucleus-targeted CNPs, their mechanisms of action in cancer-targeted diagnosis and treatment, and their applications in cancer therapy. Additionally, the article discusses the current challenges and future directions in this field, aiming to provide valuable reference information for precision cancer treatment.

Keywords: carbon nanoparticles, nucleus-targeting, tumor imaging and therapy

Introduction

Statistics indicate that the number of new global cancer cases will reach 30 million by 2040, with cancer being regarded as the second-largest health threat worldwide.[1] Traditional cancer therapies, such as chemotherapy, lack specificity to tumor cells and often result in drug resistance that caused by drug-metabolizing enzymes, exosomes, ribosomes, neutrophils, and tumor autophagy after repeated use. Consequently, higher drug dosages are required to maintain therapeutic efficacy, potentially leading to severe side effects ranging from gastrointestinal toxicity to bone marrow suppression.[2–8] Therefore, enhancing drug concentration at the tumor site is critical for improving chemotherapeutic outcomes and reducing adverse reactions.[9,10] Furthermore, the overall survival rate of cancer patients largely depends on the early identification of cancer cells and timely monitoring of treatment efficacy post-therapy.[11,12] Achieving visualization of tumor tissues or even individual cancer cells can significantly aid in diagnosis, treatment, and prognosis.[13,14]

With the emergence of nanomedicine, new opportunities have arisen for the precise diagnosis and treatment of cancer.[15] Nanoparticles can be used to create targeting drug delivery systems or probes that specifically target tumor cells, thereby reducing the toxic side effects associated with randomly dispersed drugs.[16] Additionally, these systems enable targeting imaging of tumor cells, which enhances the accuracy of imaging.[17]

Received: 31 January 2025
Accepted: 19 June 2025
Published: 5 August 2025

Although drug delivery systems or probes targeting tumor cells can overcome issues such as poor drug specificity and low bioavailability in conventional drug delivery, the shift in disease understanding from the cellular level to the subcellular organelle level has gradually made organelle-targeted imaging and therapy a research focus.[18,19] This strategy can significantly increase drug concentration within sensitive organelles, disrupt their microstructures, induce organelle dysfunction, and ultimately lead to the lysis and death of cancer cells. Compared to delivering drugs to tumor cells, organelle-targeted strategies can provide superior therapeutic effects.[20,21] However, among current delivery systems, only a few can achieve targeting of the cell nucleus.[22–26] In fact, the cell nucleus is the ultimate target for most anticancer drugs, which exert their effects by interacting with DNA or inhibiting topoisomerase activity to disrupt DNA structure, thereby affecting replication and transcription processes.[27–29] Additionally, changes in the organization of nucleus structures are closely related to disease phenotypes, and precise imaging of the nucleus can provide critical information for disease diagnosis and treatment. Therefore, targeted imaging and therapy of the cell nucleus represent important means to further enhance therapeutic efficacy.[30]

In recent years, the integration of nanomedicinal carriers, chemotherapeutic agents, and nucleus targeting modifiers to develop nucleus-targeting nanomedicine delivery systems has demonstrated remarkable efficacy in anti-tumor research.[31] The preparation of nanocarriers and precise nucleus targeting are two critical steps for nucleus-targeting nanomedicine delivery systems. Currently, the main nanocarriers used for targeting include gold nanoparticles, silica nanoparticles, carbon nanoparticles (CNPs), polymeric nanoparticles, micelles, and liposomes.[32] Among them, carbon nanoparticles include fullerenes, carbon nanotubes (CNTs), mesoporous carbon nanospheres (MCNs), graphene, and carbon dots (CDs) (as shown in Figure 1), possessing several advantages such as simple preparation processes, excellent stability, superior mechanical, thermal, and optical properties, good biocompatibility, and effective drug-loading capacity. Their favorable water solubility also enables them to deliver drugs with poor water solubility to the target site.[33–37] Additionally, the

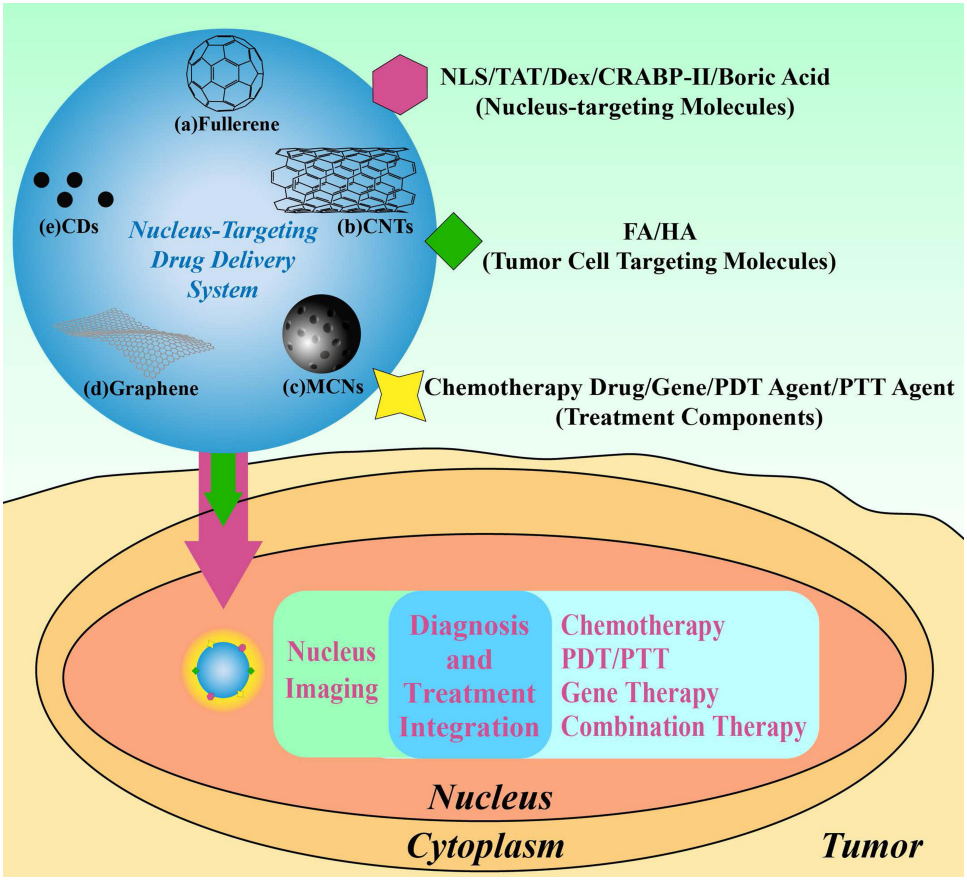

Figure 1 Strategies for construction of nucleus-targeting drug delivery system based on CNPs for imaging and therapy.

abundant bonding sites on their surfaces facilitate modifications with amino and carboxyl groups, enabling the conjugation of drugs and targeting molecules, thereby enhancing drug targeting. Simultaneously, CNPs can utilize their intrinsic in-situ fluorescence to monitor physiological activities and achieve visual tracking, thus synchronizing tumor therapy and monitoring.[38]

Currently, the research and development of CNPs are progressing rapidly, showing great potential for the future. However, there is a lack of detailed and systematic descriptions specifically focused on nucleus-targeting CNPs. Comprehensive summaries are beneficial for researchers to quickly understand the latest advancements in this field, which can guide the innovative development of nucleus-targeting CNPs drug delivery systems. This article begins with the nucleus targeting mechanisms of nanomaterials, focusing on CNPs carriers, and introduces the synthesis, structure, and properties of nucleus-targeting CNPs drug delivery system. Furthermore, it summarizes the factors influencing both active and passive targeting. Subsequently, it elucidates the applications of nucleus-targeting CNPs in tumor imaging and therapy. Finally, it addresses existing challenges and prospects for future developments.

Mechanism of Targeting the Cell Nucleus

In order to achieve targeting therapy and imaging of the cell nucleus, nanoparticles (NPs) that carry therapeutic components such as chemotherapeutic agents, genes, or reagents must sequentially target tumor tissue, cells, and ultimately the cell nucleus. This process involves four critical stages (as illustrated in Figure 2): I) passive targeting and accumulation in tumor tissue; II) targeting of tumor cells; III) internalization of the cell membrane; IV) targeting of the cell nucleus.

Passive Targeting and Accumulation of NPs in Tumor

The enhanced permeability and retention (EPR) effect is the primary passive targeting mechanism for the transportation of NPs to tumor tissues.[38] Once intravenously injected into the body, NPs loaded with therapeutic components passively migrate toward blood vessels in conjunction with the blood flow, ultimately reaching and accumulating in tumor tissues (as depicted in Figure 2I).[39] Solid tumor tissues display significant anatomical and pathological disparities in comparison

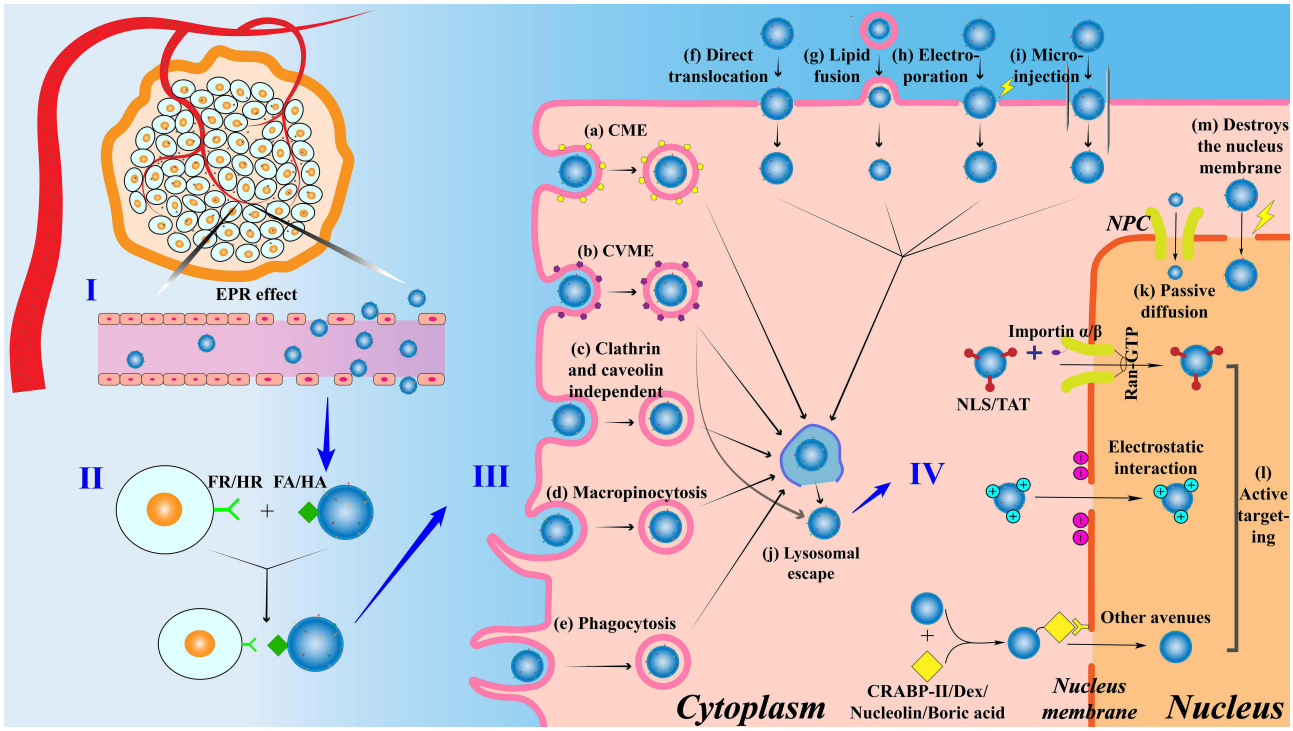

Figure 2 The targeting nucleus mechanism of NPs.

https://doi.org/10.2147/IJN.S520205

with normal tissues. As the tumor diameter expands to 1.0–2.0 mm, the tumor vasculature undergoes rapid and disordered proliferation to acquire nutrients and oxygen, leading to the formation of numerous large endothelial gaps and structurally incomplete vessels within the solid tumor tissue. Furthermore, the absence of lymphatic vessels in tumor tissues results in impaired lymphatic drainage. These two factors collectively facilitate the accumulation of NPs by the EPR effect in tumor tissues without rapid clearance from the circulation.[40,41] Conversely, in normal tissues, NPs are unable to easily penetrate the vessel walls owing to the tight junctions between vascular endothelial cells and the intact structure of the vessel walls, thus negating the manifestation of the EPR effect.

Upon reaching the tumor stroma, the surface receptors of NPs specifically bind to particular ligands on the surface of tumor cells, facilitating the aggregation of NPs from the tumor stroma to the parenchymal cells, thereby ensuring the subsequent cellular uptake of NPs.

Targeting Tumor Cells

The high affinity of ligand-receptor mediated targeting to cancer cells serves as the secondary active targeting mechanism for NPs. Prior to cellular internalization, to achieve a more precise level of targeting cancer cells, the surface of NPs can be modified with specific biomolecular ligands that bind to corresponding receptors on the surface of cancer cells, thereby promoting the cellular uptake of NPs.[42] For instance, folic acid (FA) or hyaluronic acid (HA) can recognize and bind to overexpressed folate receptors (FR) or hyaluronic acid receptors (HR) on the surface of cancer cells (as shown in Figure 2II).[43–46] Following ligand-receptor binding, NPs can actively and precisely target the surface of tumor cells and subsequently enter the cells via endocytosis, which is crucial for subsequent nucleus targeting imaging and therapy.

Intracellularization

Upon the specific binding of targeting ligands to receptors on the cell membrane, NPs proceed to the next stage, which is cellular internalization. This process is primarily mediated by the cell membrane, as shown in Figure 2III.[47] The cell membrane acts as a barrier between cells and also serves as a regulatory gateway for the movement of substances between the intracellular and extracellular environments.[48] Generally, the cellular uptake mechanisms of NPs can be categorized into two main types: endocytosis (as illustrated in Figure 2a–e) and direct entry (as depicted in Figure 2f–i).[49]

Endocytosis refers to the process through which NPs enter the interior of a cell by causing deformation of the plasma membrane. This process is classified based on the size of the vesicles formed into pinocytosis (as depicted in Figure 2a–d) and phagocytosis (as depicted in Figure 2e). Pinocytosis typically involves the uptake of NPs through small vesicles (diameter < 0.15 μm), whereas phagocytosis occurs via large vesicles known as phagosomes (diameter usually > 0.25 μm) to ingest NPs.[50] During pinocytosis, the cell membrane locally invaginates, forming small vesicles known as endosomes that can encapsulate NPs. These NPs are then transported from the extracellular matrix into the cytoplasm.[51,52] This active endocytic process can be further classified into clathrin-mediated endocytosis (CME) (Figure 2a), caveolin-mediated endocytosis (CVME) (Figure 2b), clathrin/caveolin-independent endocytosis (Figure 2c), and macropinocytosis (Figure 2d), with CME and CVME being the most common.[53]

CME relies on receptor-specific uptake and non-specific adsorption to transport NPs from the cell surface to the interior.[54] This process can be broadly divided into four steps: 1) The ligand binds to the membrane receptor, leading to the accumulation of clathrin beneath the membrane; 2) The cell membrane bends and invaginates, resulting in the formation of clathrin-coated vesicles; 3) The vesicles are cleaved and separated from the cell membrane, forming intracellular vesicles; 4) The clathrin coat is removed from the intracellular vesicles, and clathrin is recycled.[55] The average diameter of the endocytic vesicles formed is approximately 100 nm, which represents the upper size limit for NPs that can be internalized via this pathway.[56] After entering the cell through CME, NPs are typically sequestered by lysosomes.[48]

CVME is an internalization pathway that is specific to receptors and separate from CME. In this pathway, NPs are enclosed within vesicles coated with caveolin (with an average diameter of 50–80 nm) and taken up by the cell.[57] NPs that enter the cell through CVME are also captured by lysosomes, although a small number can avoid lysosomes and move directly to the next stage (organelle targeting). CVME plays a vital role in the uptake by cells, intracellular transport, and penetration into tissues by NPs.[58]

NPs can also gain entry into the cytoplasm by directly crossing the cell membrane through various methods, including biochemical or physical mechanisms. These methods include direct translocation into the cytoplasm (Figure 2f), lipid fusion into the cytoplasm (Figure 2g), electroporation strategies (Figure 2h), and microinjection strategies (Figure 2i).[59,60]

After entering the cell, the majority of NPs need to escape from endosomes or lysosomes in order to avoid degradation (Figure 2j).[61] Currently, there are four main pathways for lysosomal escape that have been documented in the literature: pore formation in the endosomal or lysosomal membrane, the proton sponge effect, membrane fusion, and photochemical disruption of the endosomal or lysosomal membrane.[62,63] Researchers have demonstrated that NPs that enter cells through the CVME pathway can sometimes evade lysosomal degradation, which is beneficial for the delivery of degradable materials such as genes and proteins.[64–66]

Nucleus Inputting Mechanism

The nucleus is separated from the cytoplasm by the nucleus envelope, which is a double membrane that contains numerous nucleus pore complexes (NPC).[67] The NPC serves as the only pathway for bidirectional exchange between the nucleoplasm and cytoplasm, and it can be divided into three layers: the luminal ring, the central scaffold, and the phenylalanine-glycine nucleoporins (FG Nups). FG Nups are arranged along the inner surface of the NPC, creating a selective barrier for nucleocytoplasmic transport.[68] There are three main pathways for NPs to pass through the NPC (Figure 2IV): 1) passive diffusion (Figure 2k); 2) active targeting (Figure 2l); 3) disruption of nucleus membrane permeability (Figure 2m).[69]

Passive Diffusion

NPs have been widely recognized for their ability to accumulate effectively in solid tumors by freely diffusing in the bloodstream and reaching the interstitial space through the EPR effect.[70] Likewise, NPs can enter the cell nucleus by freely diffusing through nucleus pores. However, owing to the restricted diameter of nucleus pores, NPs with a diameter exceeding 10 nm cannot passively diffuse into the nucleus, and this diffusion process lacks a specific direction. NPs larger than 10 nm enter the nucleus through alternative mechanisms.[71]

Active Targeting

Larger NPs face a substantial resistance barrier from the NPC and experience noticeable hindrance. However, active nucleus transport of these NPs can be accomplished by modifying their surface through ligand modification or surface charge control.

Ligand Modification

Surface ligand modification is the main strategy for constructing targeting NPs that are larger than the size of the NPC for entry into the nucleus.[72] Nucleus targeting peptides are short sequences of basic amino acids that act as signaling segments attached to nucleus import carriers. They facilitate the translocation of NPs from the cytoplasm to the nucleus through the importin pathway.[73] Nucleus targeting peptides can be classified into two types, depending on the proteins involved in the nucleus entry process: nucleus localization signal (NLS) and trans-activating transcriptional activator (TAT) peptide.

The NLS peptide, which consists of seven amino acids, was discovered by researchers during their study of the simian virus 40 T antigen.[74] The process of NLS being transported into the nucleus can be divided into four steps, as depicted in Figure 3: 1) The NLS on the NLS receptor (importin α/β dimer) forms a receptor complex; 2) The receptor complex binds to the fibrils on the NPC, creating a hydrophilic channel for the NLS to pass through; 3) Upon entering the nucleus, importin β binds to Ran-GTP (a small GTPase that can bind either GTP or GDP), causing the dissociation of the NLS and the receptor complex; 4) The receptor complex is exported from the nucleus by Ran-GTP, while Ran-GTP is converted to Ran-GDP and returns to the cytoplasm.[75]

Another peptide that targets the nucleus is TAT peptide, which aids in the translocation of NPs by binding to importin β. TAT peptide is composed of an 86-amino acid peptide, containing a highly basic region that plays a role in nucleus localization. This region consists of 9 residues, including 2 lysines and 6 arginines, and is easily recognized by the NPC, actively facilitating the delivery of NPs to the nucleus.[76,77]

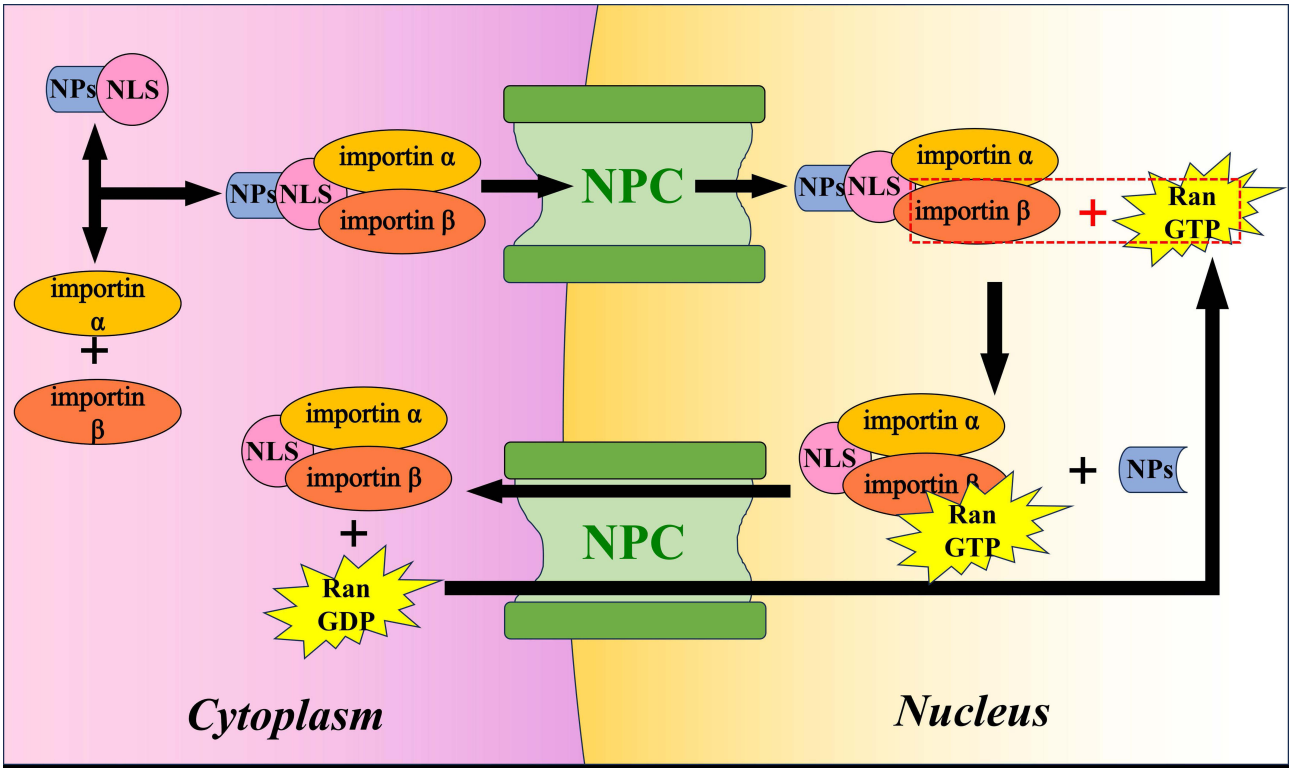

Figure 3 Schematic representation of NPs translocating into the nucleus through NLS.

Furthermore, numerous NPs can also be transported to the nucleus when they are bound to specific molecules. For example, retinol-binding protein II (RBP II), which is a cytoplasmic protein, can bind to retinoic acid to form a complex. This complex subsequently associates with importin α, facilitating its entry into the nucleus through the NPC.[78] Dexamethasone, when it binds to the glucocorticoid receptor to form a complex, can induce the expansion of the nucleus pore to 60 nm.[79] This expansion allows molecules smaller than 60 nm to enter the nucleus. Boronic acid-conjugated NPs can also achieve nucleus targeting through a different mechanism. The exposed boronic acid can bind to glucosamine residues present on nucleoporin 62 (NUP62), which is the only glycoprotein located in the inner ring of the NPC. This binding enables NPs to target the nucleus via the NPC.[80] Nucleolin, which is a shuttling protein capable of transporting from the cytoplasm to the nucleus, possesses the ability to carry NPs into the nucleus. Several ligands, including AS1411 aptamer, F3 peptide, and multivalent pseudopeptide N6L, can recognize nucleolin and have been utilized in the development of nucleus-targeting drug delivery systems.[81,82]

Surface Charge

Furthermore, the nucleus import of NPs can be facilitated by their interaction with the surface charges of the nucleus.[83] Positively charged NPs are particularly beneficial for binding to cells and the nucleus owing to the inherent negative charge of the cell membrane, which is composed of phospholipid bilayers, and the nucleic acids within the nucleus.[84] It is worth noting that NLS often consist of numerous lysine and arginine residues, which are positively charged, and this may contribute to the increased uptake capacity of NPs by the nucleus.

Disruption of Nucleus Membrane Permeability

Whether through passive diffusion or active targeting, NPs are designed to adapt to the structure and properties of the nucleus envelope in order to achieve nucleus targeting transport. Another method to facilitate the nucleus entry of NPs is to alter the rules of nucleus transport, specifically by interfering with the permeability of the nucleus membrane.[85] Disrupting the nucleus envelope allows for a wider range of drug types and sizes, as well as NPs, to enter the cell nucleus, providing a universal platform for efficient drug delivery to the nucleus. It is well known that the nucleus

envelope disassembles during mitosis, and external stimuli can also cause transient disruptions in the nucleus membrane over certain time intervals. For example, NPs loaded with photosensitizers can generate reactive oxygen species (ROS) under near-infrared (NIR) light, inducing damage to the nucleus membrane,[86] thereby allowing more NPs to enter the cell nucleus and enhancing the efficiency of photodynamic conversion.

CNPs Drug Carriers

CNPs can be chemically linked to drugs using covalent bonds, such as amide, ester, and hydrazine, or through non-covalent interactions, such as electrostatic attraction, π-π stacking, hydrogen bonding, and hydrophilic interactions. These conjugations enhance the stability of the drugs in the bloodstream and improve their bioavailability in target cells.[87,88] Currently, the main CNPs utilized in drug delivery systems include fullerenes, CNTs, MCNs, Graphene, and CDs (Figure 1a–e).

Fullerene

Fullerenes demonstrate a spherical or ellipsoidal morphology, showcasing a hollow cage-like structure (as depicted in Figure 1a). They possess a significant specific surface area and distinct nonpolar characteristics.[89] By forming covalent bonds, they can encapsulate different drugs within the cage and interact with the lipids present in cell membranes. This interaction aids in the transmembrane transport of drugs and enables controlled drug delivery.[90]

The most prevalent fullerene is C_{60}, which is composed of 60 carbon atoms connected by 30 carbon double bonds. It exhibits extensive π-π conjugation, resulting in a cage-like structure. The distinctive geometric configuration and molecular topology give it notable characteristics, including a high specific surface area, small particle size, and high reactivity.[91] Raoof et al[92] developed a highly water-soluble, non-ionic, and non-cytotoxic carrier called C60-ser, which is based on fullerene. C60-ser is prepared based on Bingel additive process of C_{60}. This method increases the solubility of fullerene and its derivatives in water. They covalently conjugated C60-ser with the PF-633 fluorophore to create C60-serPF, as shown in Figure 4A. C60-serPF has the ability to transport anticancer drugs across various biological barriers, such as cell membranes and nucleus membranes.

CNTs

CNTs are composed of carbon atoms arranged in hexagonal patterns, forming one-dimensional hollow nanotubes with layers ranging from a few to several tens (as shown in Figure 1b).[98] They can be classified as single-walled CNTs (SWCNTs) and multi-walled CNTs (MWCNTs). Their unique honeycomb structure provides a high surface area relative to their volume, allowing for the incorporation of more drugs onto the surface or within the core of CNTs through both covalent and non-covalent interactions.[99] The needle-like morphology of CNTs facilitates the transmembrane penetration of drugs and their accumulation within the nucleus through the "nanoneedle" mechanism.[100]

Tsai et al[93] were the first to synthesize oxidized multi-walled carbon nanotubes (OX-MWCNTs), which were then conjugated with heparin to form Hep-MWCNTs. Subsequently, polyglycolic acid (PGA) was reacted with Hep-MWCNTs to synthesize an amphiphilic block copolymer known as PGA-Hep-MWCNTs (as depicted in Figure 4B). In this polymer system, the hydrophobic interactions between PGA and MWCNTs result in the formation of an amphiphilic copolymer. This copolymer enables the encapsulation of Doxorubicin (DOX) not only through π-π stacking interactions but also through the hydrophobic interactions between PGA and MWCNTs. Consequently, this polymer can effectively deliver DOX to the desired target site, thereby overcoming intracellular drug resistance.

MCNs

MCNs, as depicted in Figure 1c, are porous CNPs with pore sizes ranging from 2 to 50 nm. They possess a highly porous structure and a large specific surface area, which offers numerous binding or adsorption sites for drug molecules. This allows for efficient loading within a limited storage volume. Moreover, MCNs have the ability to undergo photothermal conversion and generate ROS when exposed to NIR light irradiation.[101] Due to their conjugated structure, they also exhibit fluorescence quenching capabilities.[102] As a result, MCNs have significant potential for multimodal therapy, addressing multidrug resistance, and achieving theranostic integration.[103]

 https://doi.org/10.2147/IJN.S520205

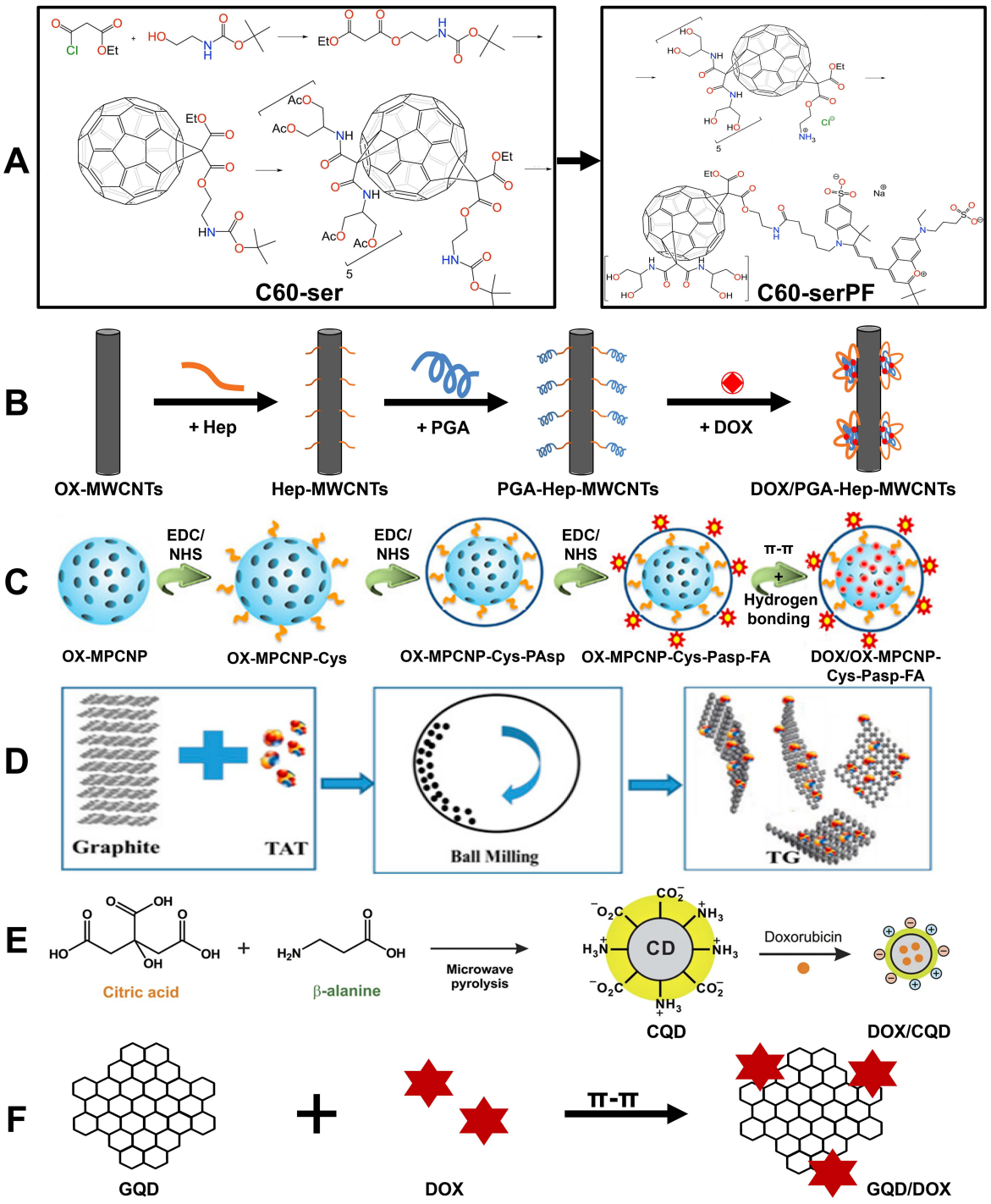

Figure 4 Synthesis route of nucleus-targeting CNPs. (**A**) Synthesis route of C60-serPF; reproduced from Raoof M, Mackeyev Y, Cheney MA, Wilson LJ, Curley SA. Internalization of C60 fullerenes into cancer cells with accumulation in the nucleus via the nuclear pore complex. Biomaterials. 2012;33:2952–2960. Copyright © 2011 Elsevier Ltd. All rights reserved.[92] (**B**) Synthesis route of DOX/PGA-Hep-MWCNTs; Reproduced from Tsai H-C, Maryani F, Huang -C-C, Imae T, Lin J-Y. Drug-loading capacity and nuclear targeting of multiwalled carbon nanotubes grafted with anionic amphiphilic copolymers. Int J Nanomed. 2013;8:4427. © 2013 The Author(s). Dove Medical Press Limited. Creative Commons Attribution - Non Commercial (unported, 3.0) License.[93] (**C**) Synthesis route of DOX/OX-MPCNP-Cys-PAsp-FA; Reproduced from Vinothini K, Dhilip Kumar SS, Abrahamse H, Rajan M. Enhanced doxorubicin delivery in folate-overexpressed breast cancer cells using mesoporous carbon nanospheres. ACS Omega. 2021;6:34532–34545. © 2021 The Authors. Published by American Chemical Society. https://creativecommons.org/licenses/by-nc-nd/4.0/.[94] (**D**) Synthesis route of TG; Reproduced from Shan S, Jia S, Lawson T, Yan L, Lin M, Liu Y. The use of TAT peptide-functionalized graphene as a highly nuclear-targeting carrier system for suppression of choroidal melanoma. Int J Mol Sci. 2019;20:4454. © 2019 by the authors. Licensee MDPI, Basel, Switzerland. This article is an open access article distributed under the terms and conditions of the Creative Commons Attribution (CC BY) license.[95] (**E**) Synthesis route of DOX/CQD; Reproduced from Jung YK, Shin E, Kim B-S. Cell nucleus-targeting zwitterionic carbon dots. Sci Rep. 2015;5. Copyright © 2015, Macmillan Publishers Limited. This work is licensed under a Creative Commons Attribution 4.0 International License.[96] (**F**) Synthesis route of GQD/DOX; Reproduced from Wang C, Wu C, Zhou X, et al. Enhancing cell nucleus accumulation and DNA cleavage activity of anti-cancer drug via graphene quantum dots. Sci Rep. 2013;3. Copyright © 2013, The Author(s). Creative Commons CC-BY-NC-ND license.[97]

Vinothini et al[94] developed a nanocarrier system based on MCNs for the targeting delivery of breast cancer drugs to the nucleus. Initially, oxidized MCNs (Ox-MPCNP) were synthesized using a hydrothermal method. Subsequently, Ox-MPCNP was conjugated with cystamine, polyaspartic acid, and folic acid (Ox-MPCNP-Cys-PAsp-FA) through EDC/NHS-mediated chemical reactions (as depicted in Figure 4C). The anticancer drug DOX was then loaded into the interior of Ox-MPCNP through π-π stacking and hydrogen bonding interactions (DOX/Ox-MPCNP-Cys-PAsp-FA). DOX/Ox-MPCNP-Cys-PAsp-FA significantly enhanced the cellular uptake of DOX via FR-mediated endocytosis, promoting greater accumulation of DOX in tumor cells and ultimately increasing the amount of DOX in the nucleus. The results confirmed the highly efficient nucleus-targeted drug delivery potential of MCNs.

Graphene

Graphene is a two-dimensional carbon nanomaterial. It is composed of carbon atoms that are arranged in a hexagonal honeycomb lattice through sp^2 hybridized orbitals. This unique arrangement gives graphene exceptional optical and mechanical properties. As a result, it has garnered considerable attention for its potential applications in biomedicine and drug delivery.[104] Graphene exhibits a significant specific surface area, as depicted in Figure 1d. This characteristic allows it to establish complexes with aromatic drugs through π-π stacking and/or hydrophobic interactions, resulting in enhanced drug storage capabilities.[105,106] Furthermore, drugs loaded onto graphene demonstrate a high level of stability, thereby preventing premature release outside the target cells. However, it is worth noting that materials based on graphene have a tendency to aggregate in buffers or cell media, which ultimately leads to a significant reduction in the surface area available for drug-loading and subsequently decreases cellular uptake. Researchers have functionalized graphene with polyethylene glycol, polyethyleneimine, gelatin, or chitosan using covalent or non-covalent strategies to achieve good dispersion and stability in physiological solutions.[107–110] Additionally, the conjugation of targeting ligands such as folic acid or TAT enhances their specific targeting capabilities, thereby improving therapeutic efficacy.[95,111]

Shan et al[95] prepared TAT-functionalized hydrophilic graphene nanosheets (TG) using an edge-functionalization ball-milling method (as depicted in Figure 4D). Following the conjugation of TAT, the hydrophobic graphene nanosheets underwent a transformation into hydrophilic polymers, thereby enhancing their ability to be transported in the bloodstream. The TG, when loaded with the chemotherapeutic drug mitomycin C, effectively penetrated both the tumor cell membrane and the nucleus membrane, showing remarkable tumor nucleus targeting capability and potent antitumor efficacy.

CDs

CDs are CNPs with a quasi-spherical morphology and dimensions smaller than 10 nm (as shown in Figure 1e).[112] Owing to their excellent optical properties, low toxicity, high water dispersibility, and affordability, CDs have gained increasing attention in the field of biomaterials.[113] The surfaces of CDs are rich in functional groups such as hydroxyl, epoxy, amino, and carboxyl groups, which enable them to load various drugs through mechanisms like electrostatic adsorption or covalent bonding. By employing nucleus targeting strategies, these drug-loaded CDs can be delivered into the nucleus of tumor cells for release, thereby achieving precise tumor cell killing while utilizing their photoluminescence properties for fluorescence imaging. This allows for the construction of an integrated platform for therapy and monitoring.[114] CDs are primarily categorized into four types: carbon quantum dots (CQDs), graphene quantum dots (GQDs), carbon nanodots, and carbonized polymer dots. Among these, CQDs and GQDs are more widely applied in drug delivery.[115]

Jung et al[96] prepared polymer CQDs using citric acid and β-alanine as raw materials through microwave-assisted pyrolysis. They subsequently loaded DOX onto the CQDs (DOX/CQD) (Figure 4E). The DOX/CQD complex was then used for cellular imaging and the delivery of DOX to the cell nucleus. GQDs are NPs of graphene that have dimensions smaller than 100 nm. They maintain the layered structural motif of graphene but have smaller lateral dimensions and a high concentration of carboxyl groups at the periphery. As a result, they demonstrate improved biocompatibility with biological systems.[116] GQDs also exhibit unique edge effects, which allow for the creation of composite materials by combining them with other substances. This characteristic makes GQDs excellent carriers for both the treatment and tracking of cancer cells. Wang et al[97] utilized graphene oxide (GO) and photo-Fenton reactions under ultraviolet irradiation to synthesize GQDs. These GQDs were subsequently conjugated with DOX through π-π interactions to

form the GQD/DOX complex for drug delivery (Figure 4F). The GQD/DOX complex demonstrated efficient delivery of DOX to the nucleus, resulting in enhanced nucleus uptake and cytotoxicity against drug-resistant cancer cells.

The Impact of Physicochemical Properties of CNPs on Nucleus-Targeting Delivery

Before entering the cell nucleus, CNPs must undergo several stages, which include circulating in the bloodstream, targeting the cell membrane, cellular uptake, and nucleus targeting. Throughout this process, the physicochemical properties of CNPs, such as their shape, size, and surface charge, have an impact on their interactions with the surrounding environment, including blood cells, the cell membrane, and the nucleus membrane. These interactions, in turn, affect the CNPs' overall performance in nucleus targeting.[117,118]

Shape

The geometric shape of CNPs has an impact on their transportation in the bloodstream and their ability to penetrate tumor tissues, which in turn affects the concentration of drugs that enter the cell nucleus. In comparison to spherical CNPs like CDs and MCNs, non-spherical CNPs such as rod-shaped CNTs and disc-shaped graphene have been found to decrease macrophage uptake, prolong circulation time in the bloodstream, and ultimately increase the number of CNPs that can penetrate from the blood into tumors.[117] Furthermore, the adhesion sequence of CNPs on the cell surface is as follows: rod-shaped > disc-shaped > spherical.[118] This makes non-spherical CNPs, particularly rod-shaped ones, advantageous for targeting cellular and nucleus structures.[119–121] However, the efficiency of cellular uptake follows a different sequence: disc-shaped > spherical > ellipsoidal.[122] Studies have indicated that spherical CNPs are primarily internalized by cells through the CVME mechanism, whereas rod-shaped CNPs tend to be internalized passively, resulting in higher cellular uptake rates for spherical CNPs.[123]

Size

The size of CNPs can impact their efficiency in endocytosis, which subsequently affects the concentration of drugs that ultimately enter the cell nucleus. The optimal size for endocytosis falls within the range of 10–100 nm. CNPs that are smaller than 10 nm experience inhibited endocytosis because of the high energy cost associated with membrane bending during the interaction between the cell and CNPs, as well as the subsequent encapsulation of CNPs by the membrane. Similarly, larger CNPs are also limited in their uptake through endocytosis because the size range of endocytic vesicles typically falls between 50–100 nm.[124] Further researches have demonstrated that among NPs within the size range of 7.5 nm to 100 nm, those with diameters of 50–60 nm are more effective in penetrating cells, thereby achieving efficient cellular uptake.[125]

CNPs with dimensions smaller than 20 nm can enter the cell nucleus via NPCs, thus necessitating appropriate adjustment of CNPs size for nucleus targeting.[126] Studies have demonstrated that anionic/cationic CNPs with dimensions less than 5 nm can more easily penetrate the cell nucleus through endocytosis or direct membrane penetration.[127–129] For example, cationic CDs have been utilized for labeling/imaging the nucleolus[127] or DNA structures within the nucleolus,[128] while anionic CDs conjugated with photosensitizers have been employed for nucleolar labeling in photodynamic therapy.[129] Su et al[130] developed a size-tunable GQDs nanovehicle (SCNA), which is composed of ultrasmall quantum dots (less than 5 nm) functionalized with pH-sensitive polymers. These polymers remain stable and inconspicuous at physiological pH but undergo aggregation transformation under the slightly acidic conditions of the tumor microenvironment. The size transition of SCNA at the tumor site is further induced by NIR radiation, which decomposes the 150 nm SCNA into 5 nm DOX (DOX)/GQD complexes, resembling a jet carrying a bomb. This facilitates penetration into deeper tumor tissues and increases drug concentration in the nucleus of tumor cells.

Surface Charge

Surface charge plays a significant role in the cellular uptake of CNPs. This is because cell membranes and nucleic acids are composed of negatively charged phospholipid bilayers. As a result, positively charged CNPs are able to more

effectively achieve cellular internalization.[131] Furthermore, the charge of CNPs also influences the uptake pathway. Negatively charged CNPs are more readily absorbed via caveolin-mediated endocytosis, while positively charged CNPs are more likely to be internalized through clathrin-mediated endocytosis.[132] The nucleolar, located within the cell nucleus, contains a high concentration of RNA. RNA has a phosphoribose backbone and bases, with the phosphate groups exposed on the molecular surface, making the entire RNA molecule negatively charged. As a result, cationic CNPs can bind to RNA. Yun et al synthesized a type of nucleus-targeting zwitterionic CDs. These CDs have positively charged surface groups, allowing them to effectively interact with the negatively charged cell membrane. This interaction enables the CDs to enter the cytoplasm through clathrin-mediated endocytosis, caveolin-mediated endocytosis, and passive diffusion. Subsequently, the CDs interact with the negatively charged cell nucleus, facilitating their nucleus translocation.[133]

The Application of CNPs in Nucleus Targeting

CNPs possess several advantages as carriers in drug delivery. These advantages include excellent biocompatibility, high drug loading capacity, good chemical stability, flexible functionalization, precise targeting, and controlled drug release. These advantages enable CNPs to deliver therapeutic molecules precisely to the cell nucleus. Simultaneously, the direct delivery of therapeutic molecules to the cell nucleus can disrupt genetic material, potentially causing DNA damage or inhibiting topoisomerases. This disruption can lead to overwinding or underwinding of DNA, which subsequently activates the caspase cascade and ultimately results in cell death.[134] Furthermore, while CNPs selectively target the cell nucleus for therapy, their inherent fluorescence allows for imaging. This fluorescence serves as a guidance and monitoring tool, thereby synergistically enhancing the efficiency of tumor treatment. The following sections provide details on various applications of CNP-based nucleus-targeting delivery systems in the treatment and imaging of tumor cells. These applications include nucleus imaging, chemotherapy, photothermal therapy, photodynamic therapy, gene therapy, combination therapy, and theranostics.

Nucleus Imaging

In eukaryotic cells, the nucleus contains the majority of genetic material and plays a crucial role in DNA replication, ribosome and mRNA synthesis, as well as gene expression.[135] Additionally, changes in the organization and structure of the nucleus are closely associated with disease phenotypes and serve as targets for multiple chemotherapeutic agents. Precise imaging of the nucleus can provide critical information for nucleus tracing, disease diagnosis, and treatment.[136] As mentioned previously, strategies for targeting the nucleus can be achieved by introducing molecules such as NLS and TAT into CNPs. Expanding on this foundation, further targeting of specific subnuclear structures, such as the nucleolar and chromatin, and even nucleic acid molecules, can enable more refined targeting imaging.

Song et al[137] utilized TAT-modified CDs (TAT-CDs) as nucleus imaging probes and validated their capability to penetrate the nucleus by employing mouse melanoma cells B16-F10 for bioimaging. After incubation with TAT-CDs, distinct fluorescence signals were observed within the nucleus of B16-F10 cells (Figure 5A), suggesting that TAT-CDs have the ability to penetrate cells and interact with the nucleus. Similarly, Yang et al[138] designed a novel type of nucleus-targeting imaging CDs by the modification of NLS (NLS-CDs). The localization of NLS-CDs in MCF7 and A549 cells was monitored using confocal laser scanning microscopy (CLSM). As depicted in Figure 5B, NLS-CDs successfully penetrated into the cell nucleus and emitted a distinct blue fluorescence after co-incubation for 4 h, thus demonstrating their potential as fluorescent probes for nucleus imaging.

The nucleolar, being a crucial constituent of the cell nucleus, is intricately linked to mitosis, cell proliferation, regulation of the cell cycle, aging, and responses to stress. Alterations in its dimensions and morphology are frequently employed as indicators for specific diseases, thereby establishing the nucleolar as a significant biomarker for the diagnosis of malignant conditions.[143] Yin et al[139] synthesized CDs with RNA-responsive functionality. The CDs contain cationic benzothiazole groups, enabling them to exhibit "turn-on" fluorescence signaling in the presence of RNA. Figure 5C demonstrates that the fluorescence intensity peaked after cells were incubated with CDs for 120 s. These findings suggest that CDs successfully enabled rapid and wash-free nucleolar imaging, which is essential for studying RNA dynamics, visually screening RNA-targeted anticancer drugs, and evaluating their effectiveness. In contrast, Hua

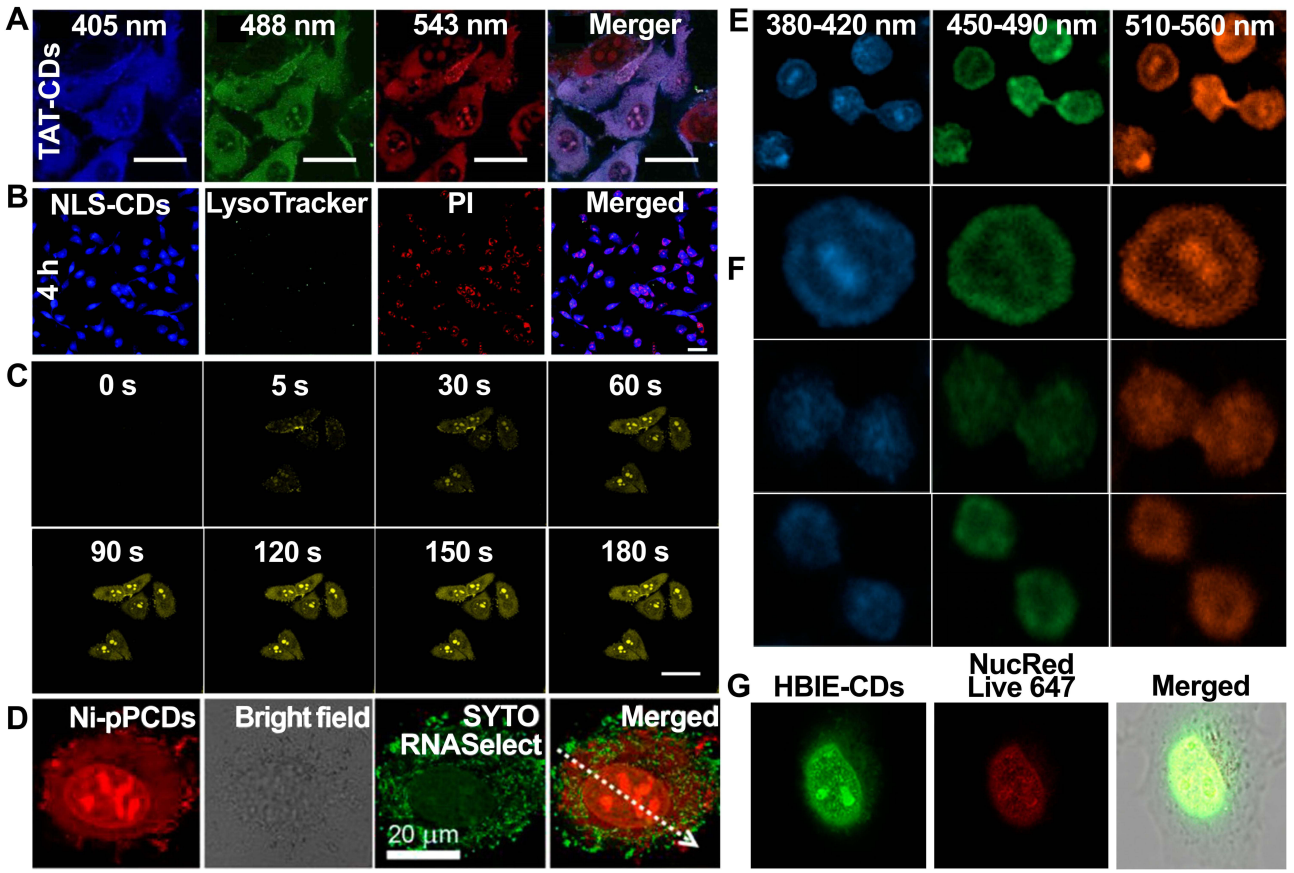

Figure 5 Images for nucleus imaging using nucleus-targeting CNPs: (**A**) CLSM images of B16-F10 cells and TAT-CDs; Reproduced from Song Y, Li X, Cong S, Zhao H, Tan M. Nuclear-targeted of TAT peptide-conjugated carbon dots for both one-and two-photon fluorescence imaging. © 2019 Elsevier B.V. All rights reserved.[137] (**B**) CLSM image of NLS-CDs incubated with MCF7 cells for 4 h; Repproduced from Yang L, Jiang W, Qiu L, et al. One pot synthesis of highly luminescent polyethylene glycol anchored carbon dots functionalized with a nuclear localization signal peptide for cell nucleus imaging. Nanoscale. 2015;7:6104–6113. Copyright 2019, Royal Society of Chemistry.[138] (**C**) CLSM images of HeLa cells incubated with CDs; Reproduced from Yin X, Sun Y, Yang R, Qu L, Li Z. RNA-responsive fluorescent carbon dots for fast and wash-free nucleolus imaging, Spectrochim. Acta A Mol Biomol Spectrosc. 2020;237:118381. © 2020 Elsevier B.V. All rights reserved.[139] (**D**) The localization of Ni-pPCDs and SYTORNASelect in cells; Reproduced from Hua X-W, Bao Y-W, Zeng J, Wu F-G. Nucleolus-targeted red emissive carbon dots with polarity-sensitive and excitation-independent fluorescence emission: high-resolution cell imaging and in vivo tracking. ACS Appl Mater Interfaces. 2019;11:32647–32658. Copyright © 2019 American Chemical Society.[140] (**E**) Asynchronous cell imaging and (**F**) polychromatic laser CLSM for HeLa cells; Reproduced from Zhang Y, Zhang X, Shi Y, Sun C, Zhou N, Wen H. The synthesis and functional study of multicolor nitrogen-doped carbon dots for live cell nuclear imaging. Molecules. 2020;25:306. © 2020 by the authors. Licensee MDPI, Basel, Switzerland. This article is an open access article distributed under the terms and conditions of the Creative Commons Attribution (CC BY) license.[141] (**G**) CLSM images of HeLa cells and HBIE-CDs; Reproduced from Liu H, Yang J, Li Z, et al. Hydrogen-bond-induced emission of carbon dots for wash-free nucleus imaging. Analy Chem. 2019;91:9259–9265. Copyright © 2019 American Chemical Society.[142]

et al[140] synthesized Ni-pPCDs by subjecting pPDA and metal ions to hydrothermal treatment. This synthesis method allowed for stimulated emission depletion imaging of live-cell nucleoli. As shown in Figure 5D, Ni-pPCDs stained the nucleosomes with bright red fluorescence, in contrast to the commercial nucleosome dye SYTO RNA, which failed to stain the nucleosomes in live cells. Thus, Ni-pPCDs possess the ability to enable real-time imaging of live-cell nucleoli.

Zhang et al[141] synthesized nitrogen-doped CQDs (N-CQDs) with the ability to target the cell nucleus. They further found that N-CQDs can be used to track individual cells or observe processes such as mitosis by labeling the cell nucleus. Fluorescence microscopy observations of HeLa cells stained with N-CQDs revealed that N-CQDs were present within the cell nucleus, displaying multicolor luminescence effects (Figure 5E). Additionally, CLSM imaging illustrated distinctive structural alterations in cells throughout the cell cycle, as depicted by the fluorescence images of individual cells (Figure 5F). When imaging asynchronous cells, it was observed that the majority of labeled cells were in interphase. However, cells undergoing mitosis were also clearly observed, suggesting that internalized N-CQDs were concentrated in the nucleus and bound to chromatin. The intensity of light varied depending on the concentration of chromatin. This study presents a novel approach for monitoring chromatin stages.

Liu et al[142] synthesized a new type of CDs (HBIE-CDs) using a hydrothermal method with meta-phenylenediamine and folic acid. These CDs demonstrated a consistent green emission in hydrogen-bonded solutions. Given the abundant presence of DNA/RNA in the cell nucleus, the nucleic acid bases can act as hydrogen bond donors. As a result, the binding of HBIE-CDs to DNA or RNA leads to a significant enhancement in the green fluorescence. When HeLa cells were incubated with HBIE-CDs, a strong fluorescence was observed in the nucleus under 405 nm excitation. This can be attributed to the high concentration of nucleic acids present in the nucleus (Figure 5G). The nucleus was further labeled with the commercial organic dye NucRedLive647, where the overlap of green fluorescence (HBIE-CDs) and red fluorescence (NucRedLive647) precisely indicates the location of DNA within the cell nucleus. This suggests that the intense green fluorescence response of HBIE-CDs towards nucleic acids makes them appropriate as a bioimaging agent for the cell nucleus without the need for washing.

Treatment

Nucleus-targeting therapy based on CNP composites has emerged as a promising approach to overcome the limitations of traditional treatment methods. This is because CNPs not only demonstrate high drug-loading efficiency but also enable controlled and sustained drug release, thereby prolonging the duration of drug action in the body, reducing dosing frequency, and minimizing side effects. Additionally, CNPs can be combined with other biomolecules or nanotechnologies to create multifunctional drug delivery systems. The cell nucleus is highly responsive to chemotherapeutic agents and hyperthermia, making it an ideal target for enhancing tumor-targeting inhibition efficiency and effectively suppressing tumor metastasis.[144,145] Therefore, CNPs can be utilized in conjunction with nucleus-targeting strategies to deliver various therapeutic components for precise chemotherapy, photothermal therapy, photodynamic therapy, gene therapy, combination therapy, and theranostics, thereby improving treatment efficiency by directly delivering these therapeutic components to the cell nucleus.

Chemotherapy

Chemotherapy is a primary method used to treat various types of cancer. DOX, an anthracycline chemotherapeutic agent, is commonly used in the treatment of multiple cancers. Its mechanism of action is believed to be associated with DNA damage and inhibition of nucleic acid synthesis. This implies that DOX needs to cross the cell membrane and reach the nucleus in order to induce cell death. Unfortunately, DOX is not able to differentiate between cancer cells and normal cells, often resulting in severe side effects. Furthermore, the nucleus membrane acts as a barrier, making it challenging for drugs that have entered the cytoplasm to penetrate the nucleus and exert their therapeutic effects.[146] Thanks to the excellent biocompatibility, high specific surface area, and diverse functionalization capabilities of CNPs, nucleus-targeting CNPs can achieve site-specific and quantified release of tumor-sensitive chemotherapeutic drugs within the nucleus. This is of significant importance in improving the therapeutic efficacy of solid tumors.

Biswas et al[147] synthesized a hydroxyl-functionalized fullerene cage derivative (h-FCD) by further functionalizing the hydroxyl groups on the fullerene cage. They subsequently loaded DOX to obtain Dox@h-FCD. The fluorescence imaging results of HeLa cells show that DOX accumulates within the nucleus, indicating that Dox@h-FCD can deliver DOX to the nucleus (Figure 6A). The results of the cell inhibition rate assay, as depicted in Figure 6B, indicated that Dox@h-FCD exhibited the highest efficacy in reducing cell viability, surpassing even the positive control, which is attributed to the nucleus-targeting capability of Dox@h-FCD.

Das et al[148] conjugated 17β-Estradiol (E_2) steroid macromolecules linked to polyethylene glycol (PEG) onto cell-penetrating MWCNTs and loaded them with DOX to form DOX@E_2-PEG-MWCNTs for nucleus delivery in vitro and in vivo breast cancer therapy. As illustrated in Figure 6C, the colocalization image shows intense red fluorescence of DOX@E2-PEG-MWCNTs in the cell nucleus, indicating that DOX@E2-PEG-MWCNTs achieve nucleus targeting via the estrogen receptor (ER)-mediated pathway. In in vivo antitumor experiments, the antitumor efficacy of DOX@E_2-PEG-MWCNTs was 18, 17, 5, and 2 times higher than that of the saline group, drug-free E2-PEG-MWCNTs group, free DOX group, and DOX@m-PEG-MWCNTs group, respectively (as shown in Figure 6D). After resection of the tumor, it was observed that black carbon-based particles were uniformly distributed in the tumor treated with E_2-PEG-MWCNT-DOX, demonstrating the excellent tumor selectivity of MWCNTs conjugated with E_2 (Figure 6E). This represents the

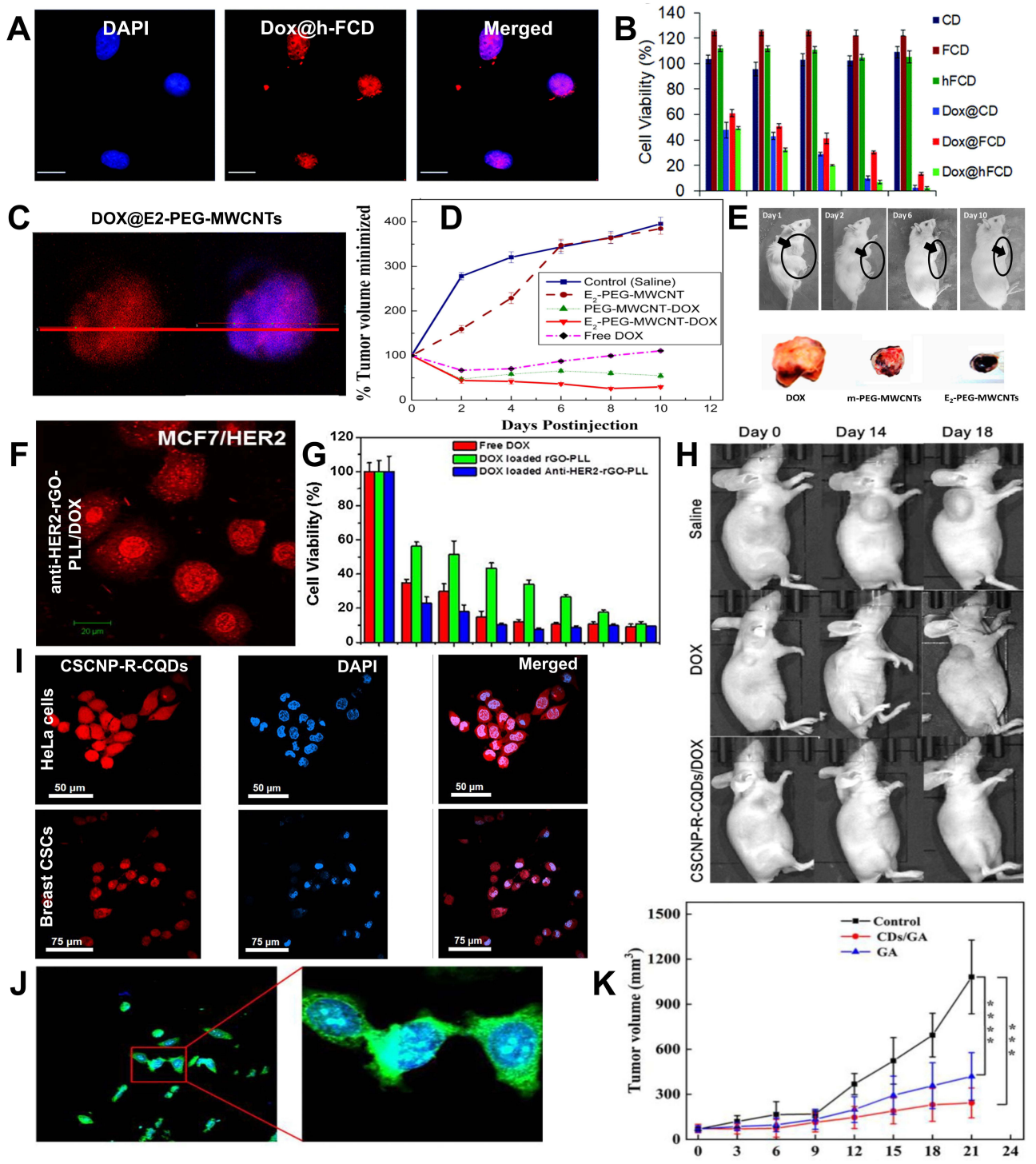

Figure 6 Images for chemotherapy using nucleus-targeting CNPs: (**A**) CLSM image of Dox@h-FCD with HeLa cells; (**B**) Viability of HeLa cells in different groups; (**C**) CLSM of MCF7 cells incubated with experimental group; (**D**) The condition of tumors post-treatment with materials from different groups; (**E**) Photographs of mouse tumors taken at different time points after treatment in the experimental group, as well as ex vivo tumor images from different groups following treatment; Das M, Singh RP, Datir SR, Jain S. Intranuclear drug delivery and effective in vivo cancer therapy via estradiol–peg-appended multiwalled carbon nanotubes. Mol Pharm. 2013;10:3404–3416. Copyright © 2013 American Chemical Society.[148] (**F**) Images of MCF7/HER2 cells incubated with experimental group; (**G**) Viability of MCF7/HER2 cells in different groups; Reproduced from Zheng XT, Ma XQ, Li CM. Highly efficient nuclear delivery of anti-cancer drugs using a bio-functionalized reduced graphene oxide. J Colloid Interf Sci. 2016;467:35–42. Copyright © 2016 Elsevier Inc. All rights reserved.[149] (**H**) Tumor conditions following the administration of different group treatments; (**I**) CLSM of CSCNP-R-CQDs incubated with HeLa cells and Breast CSCs; Reproduced from Su W, Guo R, Yuan F, et al. Red-emissive carbon quantum dots for nuclear drug delivery in cancer stem cells. J Phys Chem Lett. 2020;11:1357–1363. Copyright © 2020 American Chemical Society.[150] (**J**) CLSM images of HepG2 cells incubated with CDs; (**K**) Tumor suppression curves for CDs and CDs/GA groups; Reproduced from Liu S, Wang J, Li H, et al. Nucleus-targeting carbon quantum dots assembled with gambogic acid via π–π stacking for cancer therapy. Adv Ther. 2022;6. © 2022 Wiley-VCH GmbH.[151] ***p < 0.001, ****p < 0.0001.

first instance of using estrogen additive E_2 as a molecular transporter with MWCNTs to achieve selective nucleus delivery to cancer cells and effective in vivo breast cancer treatment.

Zheng et al[149] prepared nanocarriers by conjugating anti-HER2 antibodies with poly-L-lysine-functionalized reduced graphene oxide (anti-HER2-rGO-PLL) to efficiently deliver DOX to the nucleus of cancer cells that overexpress HER2. The anti-HER2-rGO-PLL facilitated the rapid accumulation of DOX within the nucleus, as depicted in Figure 6F. The fluorescence intensity of DOX in the nucleus was significantly higher compared with that in the cytoplasm, demonstrating the effective nucleus accumulation of DOX after the internalization of anti-HER2-rGO-PLL/DOX into MCF7/HER2 cells. In vitro cytotoxicity assays clearly revealed that the anti-HER2-rGO-PLL/DOX exhibited a sevenfold enhancement in anticancer efficacy compared with rGO-PLL/DOX (Figure 6G). These results indicate that anti-HER2-rGO-PLL is a promising carrier for the effective nucleus delivery of chemotherapeutic agents to HER2-overexpressing tumors.

Su et al[150] reported the development of red emissive CDs (CSCNP-R-CQDs) that have the ability to enter the nucleus of both cancer cells and cancer stem cells (Breast CSCs) simultaneously (Figure 6I). In vivo antitumor experiments confirmed that treatment with CSCNP-R-CQDs/DOX significantly inhibited tumor growth, while tumors treated with DOX and saline showed significant increases in volume (Figure 6H). To assess the impact of CSCNP-R-CQDs/DOX on CSCs in vivo, the percentage of CSCs (CD44+/CD24 levels) was measured in MDA-MB-231 xenograft-bearing nude mice after treatment with CSCNP-R-CQDs/DOX. After 16 days of treatment, the CD44+/CD24 levels decreased from 61.5 ± 5.6% to 10.4 ± 1.9%, which indicated that CSCNP-R-CQDs/DOX effectively targeted and eliminated CSCs, thus demonstrating its potential for inhibiting metastasis.

Liu et al[151] combined CDs, which inherently possess nucleus-targeting functionality, with gambogic acid (GA) via π-π stacking interactions (CDs/GA) to achieve nucleus-targeted drug delivery. As depicted in Figure 6J, when HepG2 cells were incubated with CDs for 24 hours, distinct green fluorescence was observed in the cell nucleus, indicating efficient nucleus entry of CDs from the cytoplasm within a short time. In vivo experiments, as illustrated in Figure 6K, it was demonstrated that the tumor volume in the CDs/GA group increased at a slower rate over 21 days compared with the control and GA groups, suggesting that the combination of chemotherapy with CDs can enhance nucleus-targeting and induce apoptosis in tumor cells.

PTT/PDT

Photothermal therapy (PTT) is a novel treatment modality that involves irradiating photothermal materials at the tumor site with extracorporeal NIR lights. This leads to localized temperature elevation and subsequent thermal ablation of tumor cells.[152] However, many materials currently used for PTT, such as gold NPs and metallic materials, still have various limitations, including large size, non-degradability, potential release of heavy metal ions, suboptimal cellular behavior (eg, low cellular uptake and endosomal/lysosomal sequestration), and/or low tumor-targeting efficiency. These limitations significantly impede their clinical translation.[153] In photodynamic therapy (PDT), the hypoxic tumor microenvironment and inherent drawbacks of photosensitizers (PSs), such as poor water solubility, low biostability, suboptimal cellular uptake, and subcellular localization, also severely affect the efficacy of PDT. Nucleus-targeting CNPs, owing to their ultrasmall size and excellent biocompatibility, can be easily eliminated via the renal clearance system. This reduces adverse clearance by the reticuloendothelial system and allows for deep penetration into tumors. When utilized for PTT or loaded with PSs for PDT, nucleus-targeting CNPs can penetrate deep into tumor tissues and act on the cell nucleus, achieving optimal PTT/PDT treatment.

Hua et al[154] mixed bovine serum albumin, CDs, and metal ions, and then loaded the mixture with PSs to synthesize a novel multifunctional nanodot called BCCGH. It was found that BCCGH has a high photothermal conversion efficiency of 68.4%, indicating its potential in PTT and PDT (Figure 7A). Upon irradiation with an 808 nm laser at 0.3 W/cm² for 10 minutes, the nucleus of cells in the BCCGH group were illuminated (Figure 7B). To investigate the cellular DNA damage induced by PDT, immunofluorescence staining was performed. The fluorescence intensity of the cell nucleus in the BCCGH + PTT + PDT group was significantly higher than that of the other groups, suggesting that PTT/PDT can enhance the cellular uptake of BCCGH and facilitate its delivery to the nucleus. Further investigation into the cellular DNA damage induced by PDT was conducted using immunofluorescence staining for phosphorylated histone H2AX on serine 139 (γ-H2AX). As shown in Figure 7B, extremely low levels of the cellular DNA damage induced by

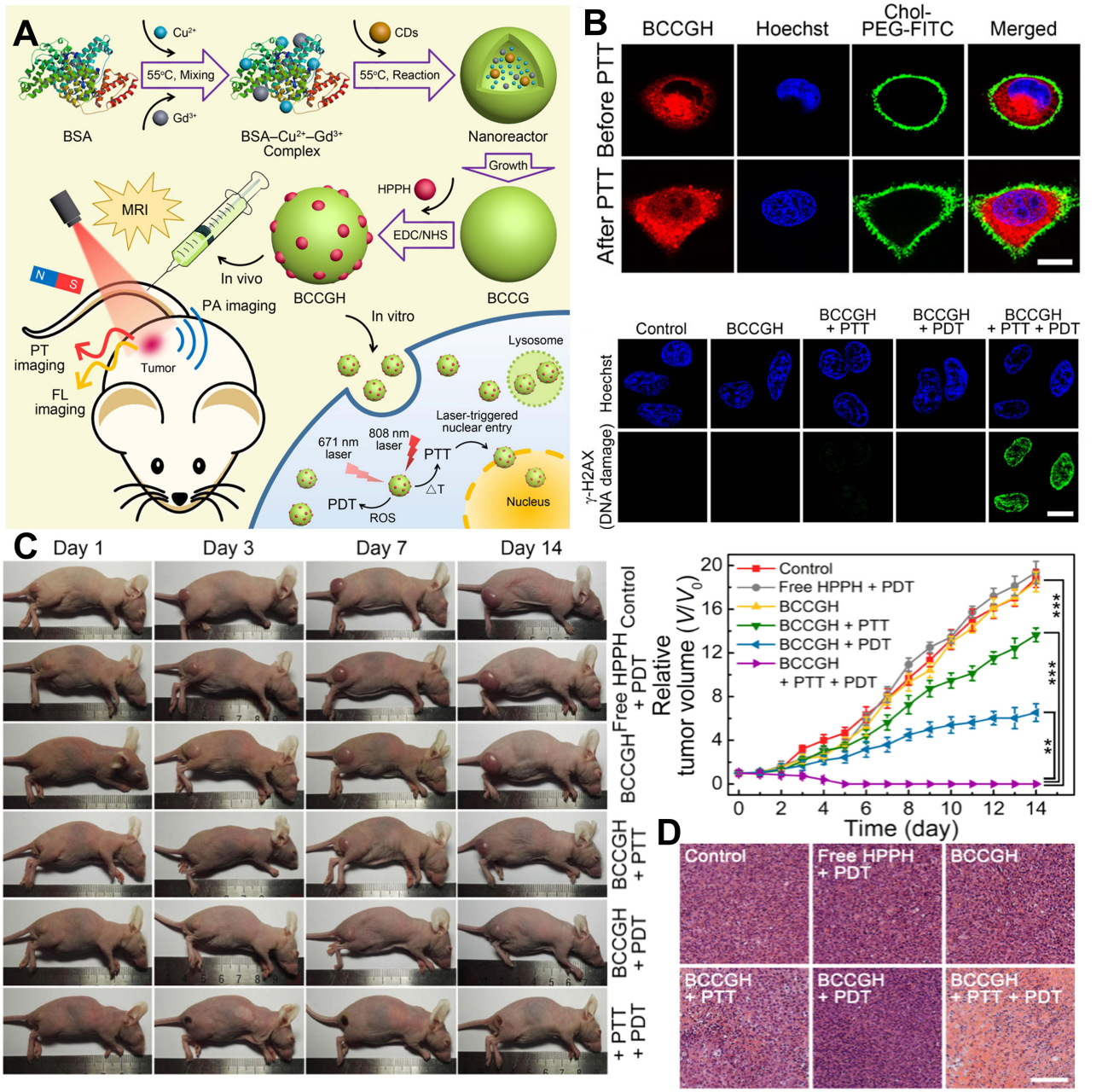

Figure 7 Images for PTT/PDT using nucleus-targeting CNPs: (**A**) The synthesis of BCCGH and its applications in PTT and PDT; (**B**) CLSM of A549 cells before and after PTT treatment, as well as CLSM of A549 cells following the various treatments indicated; (**C**) Photographs of tumor-bearing mice after the indicated treatment and a summary of tumor growth in each group. Reproduced from Hua XW, Bao YW, Zeng J, Wu FG. Ultrasmall all-in-one nanodots formed via carbon dot-mediated and albumin-based synthesis: multimodal imaging-guided and mild laser-enhanced cancer therapy. ACS Appl Mater Interfaces. 2018;10:42077–42087. Copyright © 2018 American Chemical Society.[154] **P < 0.01, ***P < 0.001; (**D**) H&E stained sections of tumor tissue.

PDT was conducted using immunofluorescence staining for phosphorylated histone H2AX on serine 139 (γ-H2AX). Combination of BCCGH with both PTT and PDT generated the highest level of DNA damage, which was attributed to the targeted nucleus PDT triggered by PTT. In vivo experiments (Figure 7C) demonstrated that tumors treated with BCCGH + PTT + PDT did not exhibit significant regrowth, indicating successful tumor elimination. This was further confirmed by hematoxylin and eosin (H&E) staining of tumor sections, which showed severe damage to the tumor tissue in the BCCGH + PTT + PDT group (Figure 7D). These findings highlight the highly efficient therapeutic potential of the synergistic PTT/PDT treatment using BCCGH, which can effectively inhibit tumor recurrence.

Gene Therapy

Gene therapy refers to the introduction of exogenous target genes into corresponding target cells by vectors, with the aim of correcting overactivated or compensating for defective genes, thereby achieving therapeutic effects for diseases. Specifically, in the context of tumor gene therapy, this involves delivering target genes into relevant target cells (such as immune cells or tumor cells) using appropriate vectors, ultimately achieving the purpose of tumor treatment. The cell nucleus, which contains most genes, is one of the effective targets for gene therapy. CQDs, a type of CDs, have gained significant attention in gene delivery applications owing to their ease of synthesis, high water solubility, biocompatibility, low toxicity, nanoscale size for cellular uptake, and luminescent properties. In particular, the dual functionality of CQDs in both bioimaging and gene delivery can greatly facilitate gene transfection. Because of their positive charge, CQDs can bind and condense negatively charged plasmids, thereby enhancing gene transfection efficiency by up to 10^4 times compared with naked plasmid delivery.[155]

The CRISPR/Cas9 system is a powerful tool for precise and programmable genome editing at specific sites in single cells and entire organisms.[156] However, the direct and efficient delivery of CRISPR/Cas9 plasmids to the cell nucleus remains a challenge.[157] Zhai et al[158] developed a nucleus-targeting gene delivery complex based on CQDs (CQD-PP), which can bypass lysosomes and enter the nucleus through passive diffusion, thereby enhancing transfection efficiency (Figure 8A). The CQD-PP was loaded with a specific sgRNA that targets the EFHD1 gene and was constructed into the CRISPR/Cas9 sgRNA plasmid pX459 (pX459-EFHD1-sgRNA). After 45 minutes of transfection in HeLa cells, the concentrated green fluorescence in the nucleus indicated successful nucleus targeting of the CQD-PP/pX459-EFHD1-sgRNA complex (Figure 8B–D). Sequencing profiles of cells transfected with CQD-PP/pX459-EFHD1-sgRNA showed overlapping peaks in the sequence trace around the Cas9 target site (Figure 8C). The indel spectrum after puromycin resistance selection indicated an editing efficiency of 34.2% in cells transfected with CQD-PP/pX459-EFHD1-sgRNA (Figure 8D). These results indicate that CQDs-PP achieved nucleus-targeting delivery of the pX459-EFHD1-sgRNA plasmid and efficient EFHD1 gene editing. In summary, CQDs-PP-mediated nucleus-targeting CRISPR/Cas9 delivery may serve as an effective tool for genome editing and fluorescence tracking.

Combination Therapy

Owing to the inherent limitations of individual therapeutic modalities, the combination of multiple treatment approaches can synergistically enhance the efficacy of tumor therapy. This approach overcomes the drawbacks of monotherapy and achieves a higher therapeutic effect. Xie et al[159] functionalized hollow carbon nitride nanospheres (HCNS) with hydroxyapatite and a mitochondria-targeting peptide (KLA), creating a delivery system that acts as PSs. After loading with DOX, it forms a complex known as HKHD. Under light irradiation, HKHD directly generates ROS, maximizing its PDT efficiency. This leads to the activation of Caspase-3 and Caspase-9, the release of Cytochrome c, and the initiation of the apoptotic cascade. The dual targeting capability of HKHD to both mitochondria and nucleus allows DOX to disrupt these organelles, thereby enhancing its antitumor activity (Figure 9A). As shown in Figure 9B, at 6 h, the red fluorescence of HKHD was observed in both mitochondria and nucleus, and the intensity of the red fluorescence increased in these organelles with the extension of time, indicating the redistribution of internalized free DOX to mitochondria and nucleus. The potential of HKHD plus light irradiation (HKHD+L) to improve antitumor efficacy was evaluated in A549 tumor-bearing mice. As depicted in Figure 9C, from 33 d to 39 d, tumor growth was significantly delayed in the HKHD and HKHD+L groups compared with the DOX, HD, and HHD groups. Moreover, the tumor tissue in the HKHD+L group exhibited a more loosely structured with increased intercellular spaces compared with the other five groups (Figure 9D). Owing to the modification with HKH, HKHD showed high tumor accumulation, primarily attributed to the EPR effect. Additionally, PDT facilitates the faster release of DOX in mitochondria and nuclei, thereby enhancing its pharmacological effects. Overall, the chemophotodynamic synergy of the dual-targeting HKHD enhanced the therapeutic outcomes, surpassing those of monotherapies.

https://doi.org/10.2147/IJN.S520205

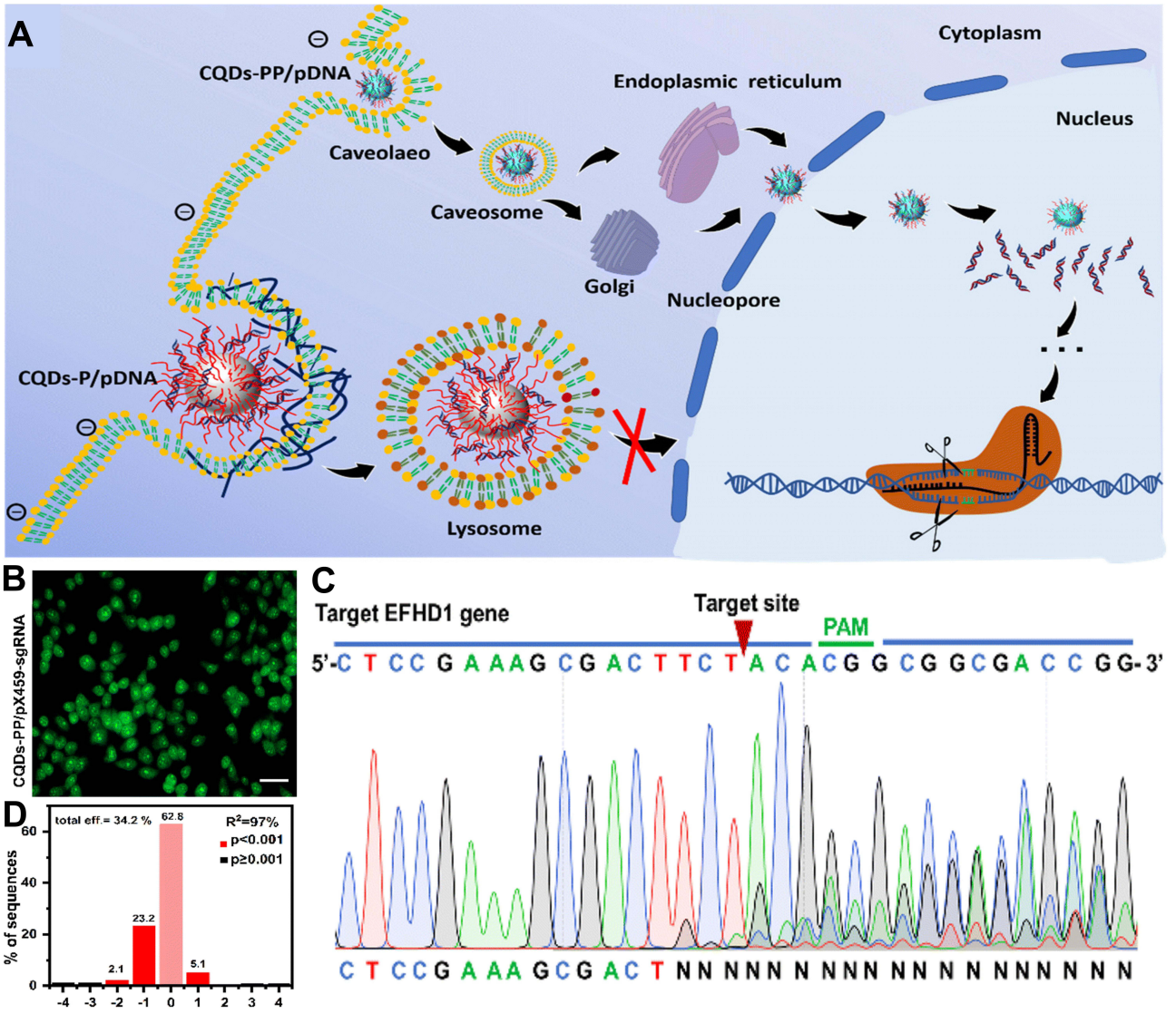

Figure 8 Images for gene therapy using nucleus-targeting CNPs: (**A**) Schematics representation of CQDs an effective tool for genome editing and fluorpDNA was taken up by cells through caveolae-mediated endocytosis. Caveosomes containing CQDsininpDNA traffic to the Golgi and/or endoplasmic reticulum (ER), which then penetrate into the cytosol, ultimately enter the nucleus via nuclear pore complexes through passive diffusion. CQDs–P/pDNA was taken up by cells through clathrin-mediated endocytosis. Endocytic vesicles would deliver CQDsivepDNA to lysosomes and thus limit their release. Even if CQDsn ipDNA escape from lysosomes, they cannot enter the nucleus through NPCs due to exceeding the threshold diameter for passive diffusion; (**B**) Confocal laser scanning microscopy images of pX459-EFHD1-sgRNA transfected into HeLa cells for 45 minutes; (**C**) Genomic DNA sequencing profile; (**D**) Indel spectrum following puromycin resistance selection. Reproduced from Zhai LM, Zhao Y, Xiao RL, et al. Nuclear-targeted carbon quantum dot mediated CRISPR/Cas9 delivery for fluorescence visualization and efficient editing. Nanoscale. 2022;14:14645–14660. Copyright 2022 Royal Society of Chemistry.[158]

Diagnosis and Treatment Integration

Materials that integrate diagnosis and therapy can accurately identify the location of tumors, and determine the most effective drug dosage and treatment duration by obtaining real-time information on the distribution of drugs within the body. CNPs not only offer distinct advantages in either therapy or imaging but also achieve the combination of diagnosis and therapy with nucleus targeting because of their exceptional fluorescence properties and modifiability, which are gaining more and more recognition.

Chen et al[160] developed a system for nucleus-targeting drug delivery using TAT-conjugated GQDs (DOX-GQDs-PEG/TAT) based on fluorescence resonance energy transfer (FRET). This system also allows for real-time monitoring of the drug release process through FRET signals (Figure 10A). The effective transport of DOX-GQDs-PEG/TAT into the cell nucleus is facilitated by both TAT and the small size of GQDs. In comparison to cells cultured with free DOX, the

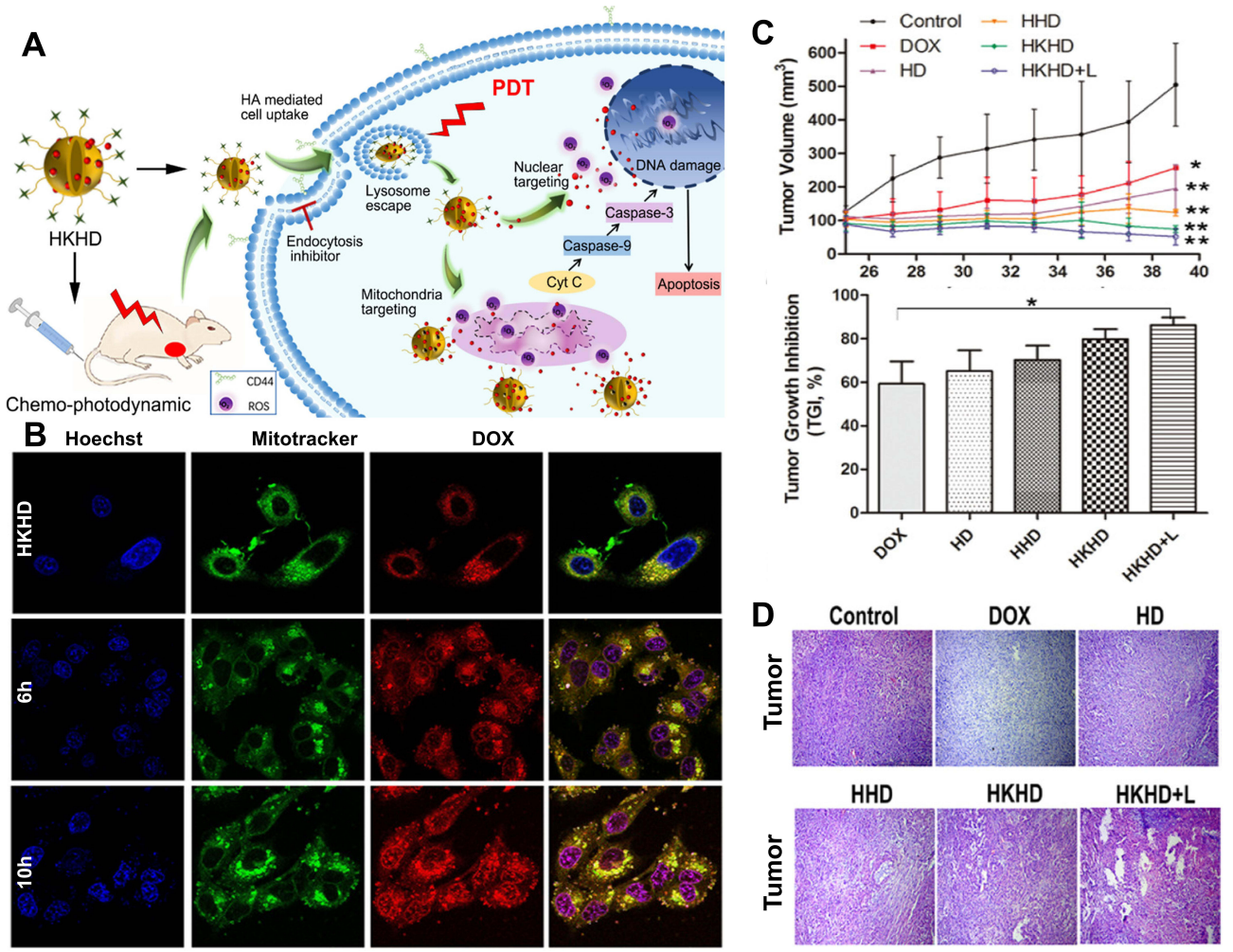

Figure 9 Images for combination therapy using nucleus-targeting CNPs: (**A**) The synthesis and synergistic therapeutic mechanism of HKHD; (**B**) CLSM images of A549 cells treated with HKHD; (**C**) The growth and inhibition of tumors following different treatments are shown. *P < 0.05; **P < 0.01; (**D**) H&E staining was used to evaluate tumor apoptosis. Reproduced from Xie R, Lian S, Peng H, et al. Mitochondria and nuclei dual-targeted hollow carbon nanospheres for cancer chemophotodynamic synergistic therapy. Mol Pharm. 2019;16:2235–2248. Copyright © 2019 American Chemical Society.[159]

amount of intranuclear accumulated drug in cells cultured with DOX-GQDs-PEG/TAT increased by 55.77% (Figure 10B). When DOX separates from the GQDs, its emission intensity decreases, while the emission intensity of the GQDs increases. Therefore, the dynamic process of DOX release can be tracked using FRET signals (Figure 10D). MTT results indicate that DOX-GQDs-PEG/TAT exhibits higher cytotoxicity towards HeLa cells (Figure 10C). TAT-conjugated GQDs show promise in targeting drug delivery, and the assembly of a FRET model between the carrier and the loading components is a precise method for tracking the drug release.

Hua et al[129] synthesized a new class of multifunctional CDs through a one-pot hydrothermal reaction of m-phenylenediamine and L-cysteine. These CDs can achieve high-quality nucleolar imaging in living cells. When CDs were conjugated with the photosensitizer protoporphyrin IX (PpIX), the resulting CDs-PpIX showed significantly enhanced cellular uptake and targeting properties, as well as improved PDT efficiency. When the amino groups of CDs are coupled with the carboxyl groups of the photosensitizer protoporphyrin IX (PpIX), the resulting CDs-PpIX exhibit significantly enhanced cellular uptake and nucleus targeting characteristics, as well as improved PDT efficiency. Figure 10E demonstrates that after incubating cells with CDs-PpIX for 12 and 18 hours, strong red fluorescence appeared in the cytosol, along with some red fluorescent spots in the nucleus. At 24 hours, a significantly greater number of red fluorescent spots were observed in the nucleus, indicating a substantial increase in PpIX cellular uptake and nucleus delivery in the CDs-PpIX group. In vivo PDT effects showed that tumors in mice treated with "CDs-PpIX + laser" were

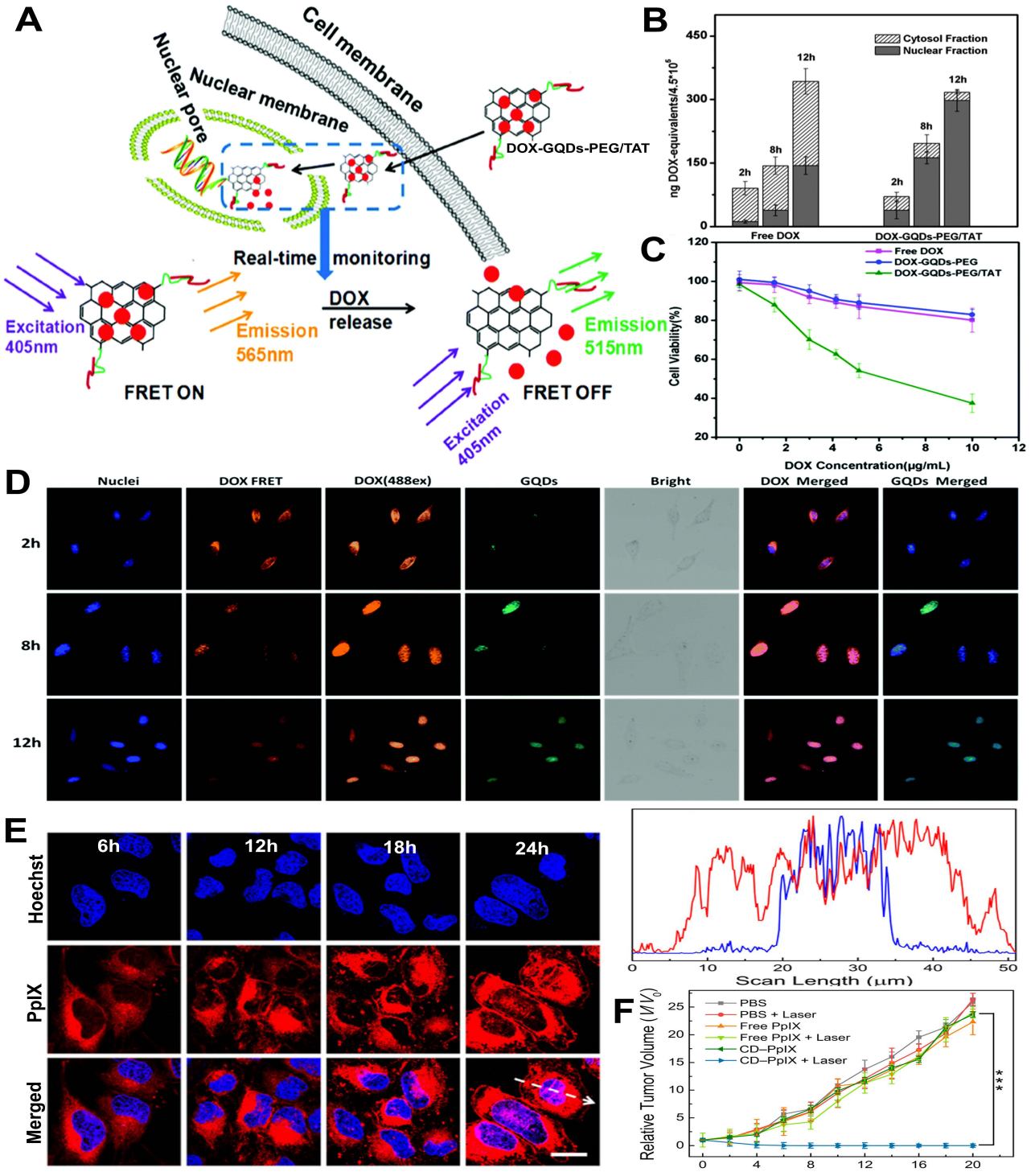

Figure 10 Images for diagnosis and treatment using nucleus-targeting CNPs: (**A**) Schematic illustration of the FRET system based on GQDs for nucleus-targeting drug delivery; (**B**) Quantitative detection of DOX after incubation of cells with the indicated materials; (**C**) Survival rate of HeLa cells incubated with the indicated materials; (**D**) Changes in FRET signals following treatment with the indicated materials; Reproduced from Chen HS, Wang Z, Zong S, et al. A graphene quantum dot-based FRET system for nuclear-targeted and real-time monitoring of drug delivery. Nanoscale. 2015;7:15477–15486. Copyright 2015 The Royal Society of Chemistry.[160] (**E**) CLSM images at different time points after treatment with CD-PpIX, and the corresponding fluorescence-intensity-profile analysis of the marked arrows in (**E**). Red line: PpIX, blue line: Hoechst 33342; (**F**) Tumor growth curves in mice after the indicated treatments; Reproduced from Hua XW, Bao YW, Wu FG. Fluorescent carbon quantum dots with intrinsic nucleolus-targeting capability for nucleolus imaging and enhanced cytosolic and nuclear drug delivery. ACS Appl Mater Interfaces. 2018;10:10664–10677. Copyright © 2018 American Chemical Society.[129] ***P < 0.001.

completely eradicated (Figure 10F), with no regrowth observed over 20 days. In contrast, the tumor volumes in other groups of mice showed rapid and sustained growth. Therefore, CDs-PpIX hold promising prospects for nucleolar imaging, nucleus-targeting drug delivery, and cancer treatment.

Conclusion and Prospect

Nucleus-targeting CNPs drug delivery systems enable targeted and controlled release transport of drugs, offering high efficacy with minimal toxicity in cancer therapy. Furthermore, delivering drugs directly into the nucleus avoids the efflux of drugs by P-glycoprotein (P-gp) on the tumor cell membrane, thereby reducing drug resistance. Additionally, the nanoscale dimensions and surface functionalization of CNPs facilitate drug penetration through biological barriers. However, these systems also face numerous challenges:

(1) Synthesis Process Optimization. The construction and synthesis of multifunctional integrated CNPs involve complex steps, requiring stepwise validation of the effective loading and functionality of each component. Moreover, specific labeling of the nucleus using pristine CNPs is challenging and typically necessitates surface modification with targeting peptides or other functional groups, which poses significant obstacles to subsequent translation and application. For instance, the nanocarrier system based on MCNs developed by Vinothini et al[82] requires multiple reaction steps to obtain the final product, and separation/purification after each step significantly reduces the final yield. Therefore, selecting simple functional materials and simplifying the composition structure of CNPs, along with employing straightforward synthetic methods such as one-pot synthesis or room-temperature stirring, could be crucial for constructing carbon materials with simple compositions but comprehensive functions, which holds great significance for enhancing the effectiveness of cancer treatment.

(2) Size Regulation. Appropriate size is a primary condition for CNPs to function as drug delivery carriers. Although most CNPs can passively target tumor tissues via the EPR effect, the optimal size range for EPR effect lies between 150–200 nm, while smaller sizes are required for entry. Currently, the size of widely used CDs is mostly around 10 nm. Larger-sized CNPs could be considered, followed by stimulation using TEM to adjust their size autonomously, improving targeting and penetration capabilities, promoting uniform distribution within tumor tissues, and enhancing overall therapeutic effects.

(3) Structural Adjustment. An appropriate surface composition is a key factor for CNPs to effectively load drugs, as a higher density of surface active sites can increase drug-loading capacity. Moreover, abundant pore structures and large specific surface areas potentially enhance the performance of CNPs in drug delivery. For example, C60 and MCNs, with their spherical structures providing large specific surface areas, exhibit enhanced drug-loading capacities. Thus, adjusting the structure of CNPs to increase their specific surface area and drug-loading capacity could improve therapeutic outcomes.

(4) Preparation of Fluorescent CNPs with Enhanced Emission Wavelengths and Fluorescence Quantum Yields (FLQY). To facilitate biological tissue imaging and treatment, achieving adequate tissue penetration depth is critical. Currently, most luminescent CNPs prepared domestically and internationally predominantly emit in the short-wavelength blue light region. Achieving near-infrared (NIR) emission from CNPs remains an urgent issue, as NIR-emitting fluorescent CNPs not only eliminate the autofluorescence of biological tissues and minimize photodamage to organisms but also enable effective deep-tissue penetration. Furthermore, enhancing the FLQY of these materials would further strengthen their advantages in targeted imaging and labeling.

(5) Therapeutic Modality Selection. Considering the limited efficacy of single therapies in cancer treatment, combining multiple therapeutic modalities to target tumors from different angles simultaneously is crucial. For example, Xie et al[159] utilized a combination of chemotherapy and photodynamic therapy, achieving synergistic effects greater than the sum of individual treatments. This integrative approach aims at comprehensive multi-level tumor eradication, thereby enhancing the overall effectiveness of cancer treatment.

Data Sharing Statement

No data was used for the research described in the article.

AuthorContributions

All authors made a significant contribution to the work reported, whether that is in the conception, study design, execution, acquisition of data, analysis and interpretation, or in all these areas; took part in drafting, revising or critically reviewing the article; gave final approval of the version to be published; have agreed on the journal to which the article has been submitted; and agree to be accountable for all aspects of the work.

Funding

This work was supported by the National Natural Science Foundation of China (82172048, U21A20378); The Science and Education Cultivation Fund of the National Cancer and Regional Medical Center of Shanxi Provincial Cancer Hospital (TD2023003, BD2023004);Shanxi Center of Technology Innovation for Controlled and Sustained Release of Nano-drugs (202104010911026); Foundational Research Project of Shanxi Province (202203021211159, 202403021221305); Shanxi Scholarship Council of China (2024-058, 2022-039); Four "Batches" Innovation Project of Invigorating Medical through Science and Technology of Shanxi Province (2023XM012); Research Project of Second Hospital of Shanxi Medical University (202302-3); and Research Project of Health Commission of Shanxi Province (2023120).

Disclosure

The authors declare that they have no known competing financial interests or personal relationships that could have appeared to influence the work reported in this paper.

References

1. Siegel RL, Miller KD, Wagle NS, Jemal A. Cancer statistics, 2023. *CA*. 2023;73:17–48. doi:10.3322/caac.21763
2. Damia G, Garattini S. The pharmacological point of view of resistance to therapy in tumors. *Cancer Treat Rev*. 2014;40:909–916. doi:10.1016/j.ctrv.2014.05.008
3. Raju B, Choudhary S, Narendra G, Verma H, Silakari O. Molecular modeling approaches to address drug-metabolizing enzymes (DMEs) mediated chemoresistance: a review. *Drug Metab Rev*. 2021;53:45–75. doi:10.1080/03602532.2021.1874406
4. Lin Z, Wu Y, Xu Y, Li G, Li Z, Liu T. Mesenchymal stem cell-derived exosomes in cancer therapy resistance: recent advances and therapeutic potential. *Mol Cancer*. 2022;21. doi:10.1186/s12943-022-01650-5
5. Ramirez JAZ, Romagnoli GG, Kaneno R. Inhibiting autophagy to prevent drug resistance and improve anti-tumor therapy. *Life Sci*. 2021;265:118745. doi:10.1016/j.lfs.2020.118745
6. Panda SS, Sahoo RK, Patra SK, Biswal S, Biswal BK. Molecular insights to therapeutic in cancer: role of exosomes in tumor microenvironment, metastatic progression and drug resistance. *Drug Discov Today*. 2024;29:104061. doi:10.1016/j.drudis.2024.104061
7. Elhamamsy AR, Metge BJ, Alsheikh HA, Shevde LA, Samant RS. Ribosome Biogenesis: a central player in cancer metastasis and therapeutic resistance. *Cancer Res*. 2022;82:2344–2353. doi:10.1158/0008-5472.can-21-4087
8. Saw PE, Chen J, Song E. ChemoNETosis: a road to tumor therapeutic resistance. *Cancer Cell*. 2023;41:655–657. doi:10.1016/j.ccell.2023.03.011
9. Chen H, Huang S, Wang H, et al. Preparation and characterization of paclitaxel palmitate albumin nanoparticles with high loading efficacy: an in vitro and in vivo anti-tumor study in mouse models. *Drug Deliv*. 2021;28:1067–1079. doi:10.1080/10717544.2021.1921078
10. Wu X, Wang X, Zhang H, et al. Enhanced in vivo stability and antitumor efficacy of PEGylated liposomes of paclitaxel palmitate prodrug. *Int J Nanomed*. 2024;19:11539–11560. PMID: 39544893; PMCID: PMC11561736. doi:10.2147/IJN.S488369
11. Zhang K, Fu R, Liu R, Su Z. Circulating cell-free DNA-based multi-cancer early detection. *Trends Cancer*. 2023;10. doi:10.1016/j.trecan.2023.08.010
12. Fang J, Islam W, Maeda H. Exploiting the dynamics of the EPR effect and strategies to improve the therapeutic effects of nanomedicines by using EPR effect enhancers. *Drug Deliv Rev*. 2020;157:142–160. doi:10.1016/j.addr.2020.06.005
13. Du J, Li Q, Chen L, et al. In vitro cytotoxicity and antitumor activity of dual-targeting drug delivery system based on modified magnetic carbon by folate. *J Nanomater*. 2020;2020:1–11. doi:10.1155/2020/7147130
14. Wei R, Jiang G, Lv M, et al. TMTP1-modified indocyanine green-loaded polymeric micelles for targeted imaging of cervical cancer and metastasis sentinel lymph node *in vivo*. *Theranostics*. 2019;9:7325–7344. doi:10.7150/thno.35346
15. Lammers T. Nanomedicine tumor targeting. *Adv Mater*. 2024;36. doi:10.1002/adma.202312169
16. Chiu S-H, Gedda G, Girma WM. Rapid fabrication of carbon quantum dots as multifunctional nanovehicles for dual-modal targeted imaging and chemotherapy. *Acta Biomater*. 2016;46:151–164. doi:10.1016/j.actbio.2016.09.027
17. Yao -Y-Y, Gedda G, Girma WM, Yen C-L, Ling Y-C, Chang J-Y. Magnetofluorescent carbon dots derived from crab shell for targeted dual-modality bioimaging and drug delivery. *ACS Appl Mater Interfaces*. 2017;9:13887–13899. doi:10.1021/acsami.7b01599
18. Trybus W, Trybus E, Król T. Lysosomes as a target of anticancer therapy. *Int J Mol Sci*. 2023;24(2176):2176. doi:10.3390/ijms24032176
19. Liang B, Liu Q, Liu B, et al. A Golgi-targeted platinum complex plays a dual role in autophagy regulation for highly efficient cancer therapy. *Angew Chem Int Ed Engl*. 2023;62:e202312170. doi:10.1002/anie.202312170
20. Qiu J, Xia Y. Killing cancer cells by rupturing their lysosomes. *Nat Nanotechnol*. 2020;15:252–253. doi:10.1038/s41565-020-0639-z

21. Chen W, Luo G, Zhang X. Recent advances in subcellular targeted cancer therapy based on functional materials. *Adv Mater*. 2018;31:1802725. doi:10.1002/adma.201802725
22. Yamada Y, Hibino M, Sasaki D, Abe J, Harashima H. Power of mitochondrial drug delivery systems to produce innovative nanomedicines. *Adv Drug Deliv Rev*. 2020;154-155:187. doi:10.1016/j.addr.2020.09.010
23. Bhowmira R, Kyoung S, Paramesh J, et al. Nanomaterial designing strategies related to cell lysosome and their biomedical applications: a review. *Biomaterials*. 2019;211:25–47. doi:10.1016/j.biomaterials.2019.05.002
24. Li H, Zhang P, Luo J, et al. Chondroitin sulfate-linked prodrug nanoparticles target the Golgi apparatus for cancer metastasis treatment. *ACS Nano*. 2019;13:9386–9396. doi:10.1021/acsnano.9b04166
25. Shao X, Meng C, Song W, Zhang T, Chen Q. Subcellular visualization: organelle-specific targeted drug delivery and discovery. *Adv Drug Deliv Rev*. 2023;199:114977. doi:10.1016/j.addr.2023.114977
26. Shim G, Youn YS. Precise subcellular targeting approaches for organelle-related disorders. *Adv Drug Deliv Rev*. 2024;212:115411. doi:10.1016/j.addr.2024.115411
27. Corman A, Sirozh O, Lafarga V, Fernandez-Capetillo O. Targeting the nucleolus as a therapeutic strategy in human disease. *Trends Biochem Sci*. 2023;48:274–287. doi:10.1016/j.tibs.2022.09.006
28. Goyal P, Malviya R. Advances in nuclei targeted delivery of nanoparticles for the management of cancer. *Biochim Biophysi Acta*. 2023;1878:188881. doi:10.1016/j.bbcan.2023.188881
29. Zhong X, Wei G, Liu B, et al. Polyhedral oligomeric silsesquioxane-based nanoparticles for efficient chemotherapy of glioblastoma. *Small*. 2023;19. doi:10.1002/smll.202207248
30. Du W, Zhang L, Li X, Ling G, Zhang P. Nuclear targeting subcellular-delivery nanosystems for precise cancer treatment. *Int J Pharm*. 2022;619:121735.
31. Tiwari R, Jain P, Asati S, Haider T, Soni V, Pandey V. State-of-art based approaches for anticancer drug-targeting to nucleus. *J Drug Deliv Sci Tec*. 2018;48:383–392. doi:10.1016/j.jddst.2018.10.011
32. Cohen EN, Kondiah PPD, Choonara YE, du Toit LC, Pillay V. carbon dots as nanotherapeutics for biomedical application. *Curr Pharm Des*. 2020;26:2207–2221. doi:10.2174/1381612826666200402102308
33. Shi J, Wang B, Wang L, et al. Fullerene (C_{60})-based tumor-targeting nanoparticles with "off-on" state for enhanced treatment of cancer. *J Control Release*. 2016;235:245–258. doi:10.1016/j.jconrel.2016.06.010
34. Sajjadi M, Nasrollahzadeh M, Jaleh B, Soufi GJ, Iravani S. Carbon-based nanomaterials for targeted cancer nanotherapy: recent trends and future prospects. *J Drug Target*. 2021;29:1–26. doi:10.1080/1061186x.2021.1886301
35. Tang L, Li J, Pan T, et al. Versatile carbon nanoplatforms for cancer treatment and diagnosis: strategies, applications and future perspectives. *Theranostics*. 2022;12:2290–2321. doi:10.7150/thno.69628
36. Krasley AT, Li E, Galeana JM, Bulumulla C, Beyene AG, Demirer GS. Carbon nanomaterial fluorescent probes and their biological applications. *Chem Rev*. 2024;124:3085–3185. doi:10.1021/acs.chemrev.3c00581
37. Praseetha PK, Litany RJ, Alharbi HM, et al. Green synthesis of highly fluorescent carbon quantum dots from almond resin for advanced theranostics in biomedical applications. *Sci Rep*. 2024;14. doi:10.1038/s41598-024-75333-0
38. Ikeda-Imafuku M, Wang LL-W, Rodrigues D, Shaha S, Zhao Z, Mitragotri S. Strategies to improve the EPR effect: a mechanistic perspective and clinical translation. *J Control Release*. 2022;345:512–536. doi:10.1016/j.jconrel.2022.03.043
39. Hashida M. Advocation and advancements of EPR effect theory in drug delivery science: a commentary. *J Control Release*. 2022;346:355–357. doi:10.1016/j.jconrel.2022.04.031
40. Lahooti B, Akwii RG, Zahra FT. Targeting endothelial permeability in the EPR effect. *J Control Release*. 2023;361:212–235. doi:10.1016/j.jconrel.2023.07.039
41. Shi Y, van der Meel R, Chen X, Lammers T. The EPR effect and beyond: strategies to improve tumor targeting and cancer nanomedicine treatment efficacy. *Theranostics*. 2020;10:7921–7924. doi:10.7150/thno.49577
42. Gupta B, Poudel BK, Ruttala HB, et al. Hyaluronic acid-capped compact silica-supported mesoporous titania nanoparticles for ligand-directed delivery of doxorubicin. *Acta Biomater*. 2018;80:364–377. doi:10.1016/j.actbio.2018.09.006
43. Alshaer W, Hillaireau H, Fattal E. Aptamer-guided nanomedicines for anticancer drug delivery. *Adv Drug Deliv Rev*. 2018;134:122–137. doi:10.1016/j.addr.2018.09.011
44. Ashrafizadeh M, Mirzaei S, Gholami MH, et al. Hyaluronic acid-based nanoplatforms for Doxorubicin: a review of stimuli-responsive carriers, co-delivery and resistance suppression. *Carbohydr Polym*. 2021;272:118491. doi:10.1016/j.carbpol.2021.118491
45. Su X, Chan C, Shi J. A graphene quantum dot@Fe 3 O 4 @SiO 2 based nanoprobe for drug delivery sensing and dual-modal fluorescence and MRI imaging in cancer cells. *Biosens Bioelectron*. 2017;92:489–495. doi:10.1016/j.bios.2016.10.076
46. Li J, Li M, Tian L, et al. Facile strategy by hyaluronic acid functional carbon dot-doxorubicin nanoparticles for CD44 targeted drug delivery and enhanced breast cancer therapy. *Int J Pharm*. 2020;578:119122. doi:10.1016/j.ijpharm.2020.119122
47. Behzadi S, Serpooshan V, Tao W, et al. Cellular uptake of nanoparticles: journey inside the cell. *Chem Soc Rev*. 2017;46:4218–4244. doi:10.1039/c6cs00636a
48. Donahue ND, Acar H, Wilhelm S. Concepts of nanoparticle cellular uptake, intracellular trafficking, and kinetics in nanomedicine. *Adv Drug Deliv Rev*. 2019;143:68–96. doi:10.1016/j.addr.2019.04.008
49. Cong VT, Houng JL, Kavallaris M, Chen X, Tilley RD, Gooding JJ. How can we use the endocytosis pathways to design nanoparticle drug-delivery vehicles to target cancer cells over healthy cells? *Chem Soc Rev*. 2022;51:7531–7559. doi:10.1039/D1CS00707F
50. Chu Z, Wang W, Zheng W, et al. Biomaterials with cancer cell-specific cytotoxicity: challenges and perspectives. *Chem Soc Rev*. 2024;53:8847–8877. doi:10.1039/d4cs00636d
51. Ji Y, Wang Y, Wang X, et al. Beyond the promise: exploring the complex interactions of nanoparticles within biological systems. *J Hazard Mater*. 2024;468:133800. doi:10.1016/j.jhazmat.2024.133800
52. Chen SC, Zeng NJ, Liu GY, et al. Precise control of intracellular trafficking and receptor-mediated endocytosis in living cells and behaving animals. *Adv Sci*. 2024;45:e2405568. doi:10.1002/advs.202405568
53. Sousa de Almeida M, Susnik E, Drasler B, Taladriz-Blanco P, Petri-Fink A, Rothen-Rutishauser B. Understanding nanoparticle endocytosis to improve targeting strategies in nanomedicine. *Chem Soc Rev*. 2021;50:5397–5434. doi:10.1039/d0cs01127d

54. Kaksonen M, Roux A. Mechanisms of clathrin-mediated endocytosis. *Nat Rev Mol Cell Biol*. 2018;19:313–326. doi:10.1038/nrm.2017.132
55. Rennick JJ, Johnston APR, Parton RG. Key principles and methods for studying the endocytosis of biological and nanoparticle therapeutics. *Nat Nanotechnol*. 2021;16:266–276. doi:10.1038/s41565-021-00858-8
56. Wu M, Wu X. A kinetic view of clathrin assembly and endocytic cargo sorting. *Curr Opin Cell Biol*. 2021;71:130–138. doi:10.1016/j.ceb.2021.02.010
57. Gimondi S, Vieira de Castro J, Reis RL, Ferreira H, Neves NM. On the size-dependent internalization of sub-hundred polymeric nanoparticles. *Colloids Surf B Biointerfaces*. 2023;225:113245. doi:10.1016/j.colsurfb.2023.113245
58. Alhaj-Suliman SO, Wafa EI, Salem AK. Engineering nanosystems to overcome barriers to cancer diagnosis and treatment. *Adv Drug Deliv Rev*. 2022;189:114482. doi:10.1016/j.addr.2022.114482
59. Pan J, Chiang C, Wang X, et al. Cell membrane damage and cargo delivery in nano-electroporation. *Nanoscale*. 2023;15:4080–4089. doi:10.1039/d2nr05575a
60. Yang J, Griffin A, Qiang Z, Ren J. Organelle-targeted therapies: a comprehensive review on system design for enabling precision oncology. *Signal Transduct Target Ther*. 2022;7. doi:10.1038/s41392-022-01243-0
61. Selby LI, Cortez-Jugo CM, Such GK, Johnston APR. Nanoescapology: progress toward understanding the endosomal escape of polymeric nanoparticles. *Wiley Interdiscip Rev*. 2017;9:e1452. doi:10.1002/wnan.1452
62. Desai N, Rana D, Salave S, Benival D, Khunt D, Prajapati BG. Achieving endo/lysosomal escape using smart nanosystems for efficient cellular delivery. *Molecules*. 2024;29:3131. doi:10.3390/molecules29133131
63. Joshi BS, de Beer MA, Giepmans BNG, Zuhorn IS. Endocytosis of extracellular vesicles and release of their cargo from endosomes. *ACS Nano*. 2020;14:4444–4455. doi:10.1021/acsnano.9b10033
64. Shuang E, He C, Wang J-H, Mao Q, Chen X. Tunable organelle imaging by rational design of carbon dots and utilization of uptake pathways. *ACS Nano*. 2021;15:14465–14474. doi:10.1021/acsnano.1c04001
65. Smith SA, Selby LI, Johnston APR, Such GK. The endosomal escape of nanoparticles: toward more efficient cellular delivery. *Bioconjug Chem*. 2018;30:263–272. doi:10.1021/acs.bioconjchem.8b00732
66. Degors IMS, Wang C, Rehman ZU, Zuhorn IS. Carriers break barriers in drug delivery: endocytosis and endosomal escape of gene delivery vectors. *Acc Chem Res*. 2019;52:1750–1760. doi:10.1021/acs.accounts.9b00177
67. Tammam SN, Azzazy HME, Lamprecht A. How successful is nuclear targeting by nanocarriers? *J Control Release*. 2016;229:140–153. doi:10.1016/j.jconrel.2016.03.022
68. Kim SU, Fernandez-Martinez J, Nudelman I, et al. Integrative structure and functional anatomy of a nuclear pore complex. *Nature*. 2018;555:475–482. doi:10.1038/nature26003
69. Chen S, Cao R, Xiang L, et al. Research progress in nucleus-targeted tumor therapy. *Biomater Sci*. 2023;11:6436–6456. doi:10.1039/d3bm01116j
70. Zi Y, Yang K, He J, Wu Z, Liu J, Zhang W. Strategies to enhance drug delivery to solid tumors by harnessing the EPR effects and alternative targeting mechanisms. *Adv Drug Deliv Rev*. 2022;188:114449. doi:10.1016/j.addr.2022.114449
71. Huang Y, Kou Q, Su Y, et al. Combination therapy based on dual-target biomimetic nano-delivery system for overcoming cisplatin resistance in hepatocellular carcinoma. *J Nanobiotechnology*. 2023;21. doi:10.1186/s12951-023-01840-3
72. Drescher D, Büchner T, Schrade P, et al. Influence of nuclear localization sequences on the intracellular fate of gold nanoparticles. *ACS Nano*. 2021;15:14838–14849. doi:10.1021/acsnano.1c04925
73. Lisitsyna OM, Kurnaeva MA, Arifulin EA, et al. Origin of the nuclear proteome on the basis of pre-existing nuclear localization signals in prokaryotic proteins. *Biol Direct*. 2020;15. doi:10.1186/s13062-020-00263-6
74. Fan Y, Li C, Li F, Chen D. pH-activated size reduction of large compound nanoparticles for in vivo nucleus-targeted drug delivery. *Biomaterials*. 2016;85:30–39. doi:10.1016/j.biomaterials.2016.01.057
75. Lu J, Wu T, Zhang B, et al. Types of nuclear localization signals and mechanisms of protein import into the nucleus. *Cell Commun Signal*. 2021;19. doi:10.1186/s12964-021-00741-y
76. Quan X, Sun D, Zhou J. Molecular mechanism of HIV-1 TAT peptide and its conjugated gold nanoparticles translocating across lipid membranes. *Chem Chem Phys*. 2019;21:10300–10310. doi:10.1039/c9cp01543d
77. Dong S, Zhou X, Yang J. TAT modified and lipid – PEI hybrid nanoparticles for co-delivery of docetaxel and pDNA. *Biomed Pharmacother*. 2016;84:954–961. doi:10.1016/j.biopha.2016.10.003
78. Yang Q, Wu L, Li L, Zhou Z, Huang Y. Subcellular co-delivery of two different site-oriented payloads for tumor therapy. *Nanoscale*. 2017;9:1547–1558. doi:10.1039/c6nr08200a
79. Wang H, Li Y, Bai H, et al. A cooperative dimensional strategy for enhanced nucleus-targeted delivery of anticancer drugs. *Adv Funct Mater*. 2017;27:1700339. doi:10.1002/adfm.201700339
80. Wu R, Liu J, Chen D, Pan J. Carbon nanodots modified with catechol–borane moieties for ph-stimulated doxorubicin delivery: toward nuclear targeting. *ACS Appl Nano Mater*. 2019;2:4333–4341. doi:10.1021/acsanm.9b00779
81. Morozov D, Mironov V, Moryachkov RV, et al. The role of SAXS and molecular simulations in 3D structure elucidation of a DNA aptamer against lung cancer. *Mol Ther Nucleic Acids*. 2021;25:316–327. doi:10.1016/j.omtn.2021.07.015
82. Ferrara B, Belbekhouche S, Habert D, et al. Cell surface nucleolin as active bait for nanomedicine in cancer therapy: a promising option. *Nanotechnology*. 2021;32:322001. doi:10.1088/1361-6528/abfb30
83. Vedadghavami A, Zhang C, Bajpayee AG. Overcoming negatively charged tissue barriers: drug delivery using cationic peptides and proteins. *Nano Today*. 2020;34:100898. doi:10.1016/j.nantod.2020.100898
84. Gorav G, Khedekar V, Varier GK, Nandakumar P. Role of charge in enhanced nuclear transport and retention of graphene quantum dots. *Sci Rep*. 2024;14. doi:10.1038/s41598-024-69809-2
85. Dey G, Baum B. Nuclear envelope remodelling during mitosis. *Curr Opin Cell Biol*. 2021;70:67–74. doi:10.1016/j.ceb.2020.12.004
86. Shah P, Wolf K, Lammerding J. Bursting the bubble – nuclear envelope rupture as a path to genomic instability? *Trends Cell Biol*. 2017;27:546–555. doi:10.1016/j.tcb.2017.02.008
87. Chen D, Dougherty CA, Zhu K, Hong H. Theranostic applications of carbon nanomaterials in cancer: focus on imaging and cargo delivery. *J Control Release*. 2015;210:230–245. doi:10.1016/j.jconrel.2015.04.021

88. Molaei MJ. A review on nanostructured carbon quantum dots and their applications in biotechnology, sensors, and chemiluminescence. *Talanta*. 2019;196:456–478. doi:10.1016/j.talanta.2018.12.042
89. Hou W, Shen L, Zhu Y, et al. Fullerene derivatives for tumor treatment: mechanisms and application. *Int J Nanomed*. 2024;19:9771–9797. doi:10.2147/ijn.s476601
90. Goodarzi S, Da Ros T, Conde J, Sefat F, Mozafari M. Fullerene: biomedical engineers get to revisit an old friend. *Mater Today*. 2017;20:460–480. doi:10.1016/j.mattod.2017.03.017
91. Fu C, Gong S, Lin L, Bao Y, Li L, Chen Q. Characterization and efficacy of C_{60} nano-photosensitive drugs in colorectal cancer treatment. *Biomed Pharmacother*. 2024;176:116828. doi:10.1016/j.biopha.2024.116828
92. Raoof M, Mackeyev Y, Cheney MA, Wilson LJ, Curley SA. Internalization of C60 fullerenes into cancer cells with accumulation in the nucleus via the nuclear pore complex. *Biomaterials*. 2012;33:2952–2960. doi:10.1016/j.biomaterials.2011.12.043
93. Tsai H-C, Maryani F, Huang -C-C, Imae T, Lin J-Y. Drug-loading capacity and nuclear targeting of multiwalled carbon nanotubes grafted with anionic amphiphilic copolymers. *Int J Nanomed*. 2013;8:4427. doi:10.2147/ijn.s53636
94. Vinothini K, Dhilip Kumar SS, Abrahamse H, Rajan M. Enhanced doxorubicin delivery in folate-overexpressed breast cancer cells using mesoporous carbon nanospheres. *ACS Omega*. 2021;6:34532–34545. doi:10.1021/acsomega.1c04820
95. Shan S, Jia S, Lawson T, Yan L, Lin M, Liu Y. The use of TAT peptide-functionalized graphene as a highly nuclear-targeting carrier system for suppression of choroidal melanoma. *Int J Mol Sci*. 2019;20:4454. doi:10.3390/ijms20184454
96. Jung YK, Shin E, Kim B-S. Cell nucleus-targeting zwitterionic carbon dots. *Sci Rep*. 2015;5. doi:10.1038/srep18807
97. Wang C, Wu C, Zhou X, et al. Enhancing cell nucleus accumulation and DNA cleavage activity of anti-cancer drug via graphene quantum dots. *Sci Rep*. 2013;3. doi:10.1038/srep02852
98. Gaur M, Misra C, Yadav AB, et al. Biomedical applications of carbon nanomaterials: fullerenes, quantum dots, nanotubes, nanofibers, and graphene. *Materials*. 2021;14:5978. doi:10.3390/ma14205978
99. Jiang Y, Wang C, Zhang M, et al. Study of folate-based carbon nanotube drug delivery systems targeted to folate receptor α by molecular dynamic simulations. *Int J Biol Macromol*. 2023;244:125386. doi:10.1016/j.ijbiomac.2023.125386
100. Singhal R, Orynbayeva Z, Kalyana sundaram RV. Multifunctional carbon-nanotube cellular endoscopes. *Nat Nanotechnol*. 2010;6:57–64. doi:10.1038/nnano.2010.241
101. Yin Y, Sun J, Jiang T, et al. Combined doxorubicin mesoporous carbon nanospheres for effective tumor lymphatic metastasis by multi-modal chemo-photothermal treatment in vivo. *Int J Nanomed*. 2023;18:4589–4600. doi:10.2147/ijn.s418766
102. Wang S, Wu W, Liu Y, et al. Targeted peptide-modified oxidized mesoporous carbon nanospheres for chemo-thermo combined therapy of ovarian cancer*in vitro*. *Drug Deliv*. 2022;29:1951–1958. doi:10.1080/10717544.2022.2089298
103. Zhou L, Jing Y, Liu Y, et al. Mesoporous carbon nanospheres as a multifunctional carrier for cancer theranostics. *Theranostics*. 2018;8:663–675. doi:10.7150/thno.21927
104. Jiang C, Zhao H, Xiao H, et al. Recent advances in graphene-family nanomaterials for effective drug delivery and phototherapy. *Expert Opin Drug Deliv*. 2020;18:119–138. doi:10.1080/17425247.2020.1798400
105. Song S, Shen H, Wang Y, et al. Biomedical application of graphene: from drug delivery, tumor therapy, to theranostics. *Colloids Surf B Biointerfaces*. 2020;185:110596. doi:10.1016/j.colsurfb.2019.110596
106. Sattari S, Adeli M, Beyranvand S, Nemati M. Functionalized graphene platforms for anticancer drug delivery. *Int J Nanomed*. 2021;16:5955–5980. doi:10.2147/IJN.S249712
107. Jeshvaghani PA, Pourmadadi M, Yazdian F, Rashedi H, Khoshmaram K, Nigjeh MN. Synthesis and characterization of a novel, pH-responsive sustained release nanocarrier using polyethylene glycol, graphene oxide, and natural silk fibroin protein by a green nano emulsification method to enhance cancer treatment. *Int J Biol Macromol*. 2023;226:1100–1115. doi:10.1016/j.ijbiomac.2022.11.226
108. Lee B, Gries K, Valimukhametova A, et al. In vitro prostate cancer treatment via crispr-cas9 gene editing facilitated by polyethyleneimine-derived graphene quantum dots. *Adv Funct Mater*. 2023;33. doi:10.1002/adfm.202305506
109. Hao PC, Burnouf T, Chiang CW, et al. Enhanced diabetic wound healing using platelet-derived extracellular vesicles and reduced graphene oxide in polymer-coordinated hydrogels. *J Nanobiotechnology*. 2023;21. doi:10.1186/s12951-023-02068-x
110. Ibrahim IAA, Alzahrani AR, Alanazi IM. Chitosan biopolymer functionalized with graphene oxide and titanium dioxide with Escin metallic nanocomposites for anticancer potential against colon cancer. *Int J Biol Macromol*. 2023;253:127334. doi:10.1016/j.ijbiomac.2023.127334
111. Einafshar E, Javid H, Amiri H, Akbari-Zadeh H, Hashemy SI. Curcumin loaded β-cyclodextrin-magnetic graphene oxide nanoparticles decorated with folic acid receptors as a new theranostic agent to improve prostate cancer treatment. *Carbohydr Polym*. 2024;340:122328. doi:10.1016/j.carbpol.2024.122328
112. Shen C-L, Liu H-R, Lou Q, et al. Recent progress of carbon dots in targeted bioimaging and cancer therapy. *Theranostics*. 2022;12:2860–2893. doi:10.7150/thno.70721
113. Li G, Zhang X, Fei X, et al. Chiral FA Conjugated CdTe/CdS quantum dots for selective cancer ablation. *ACS Nano*. 2022;16:12991–13001. doi:10.1021/acsnano.2c05517
114. Kong J, Wei Y, Zhou F, et al. Carbon quantum dots: properties, preparation, and applications. *Molecules*. 2024;29:2002. doi:10.3390/molecules29092002
115. Lagos KJ, García D, Cuadrado CF, et al. Carbon dots: types, preparation, and their boosted antibacterial activity by photoactivation. Current status and future perspectives. *Wiley Interdiscip Rev*. 2023;15. doi:10.1002/wnan.1887
116. Iannazzo D, Pistone A, Salamò M, et al. Graphene quantum dots for cancer targeted drug delivery. *Int J Pharm*. 2017;518:185–192. doi:10.1016/j.ijpharm.2016.12.060
117. Zhang Y, Lin R, Li H, He W, Du J, Wang J. Strategies to improve tumor penetration of nanomedicines through nanoparticle design. *Wiley Interdiscip Rev*. 2018;11. doi:10.1002/wnan.1519
118. Ju Y, Guo H, Edman M, Hamm-Alvarez SF. Application of advances in endocytosis and membrane trafficking to drug delivery. *Adv Drug Deliv Rev*. 2020;157:118–141. doi:10.1016/j.addr.2020.07.026
119. Lin J, Miao L, Zhong G, Lin C-H, Dargazangy R, Alexander-Katz A. Understanding the synergistic effect of physicochemical properties of nanoparticles and their cellular entry pathways. *Commun Biol*. 2020;3:1–10. doi:10.1038/s42003-020-0917-1

120. Bannister A, Dissanayake D, Kowalewski A, Cicon L, Bromma K, Chithrani DB. Modulation of the microtubule network for optimization of nanoparticle dynamics for the advancement of cancer nanomedicine. *Bioengineering*. 2020;7:56. doi:10.3390/bioengineering7020056
121. Ren X, Yi Z, Sun Z, et al. Natural polysaccharide-incorporated hydroxyapatite as size-changeable, nuclear-targeted nanocarrier for efficient cancer therapy. *Biomater Sci*. 2020;8:5390–5401. doi:10.1039/d0bm01320j
122. Dasgupta S, Auth T, Gompper G. Wrapping of ellipsoidal nano-particles by fluid membranes. *Soft Matter*. 2013;9:5473–5482. doi:10.1039/c3sm50351h
123. Shuang E, Xing YZ, Du S, et al. Shape control of carbon nanoparticles via a simple anion-directed strategy for precise endoplasmic reticulum-targeted imaging. *Angew Chem Int Ed Engl*. 2023;62. doi:10.1002/anie.202311008
124. Debnath K, Pal S, Jana NR. Chemically designed nanoscale materials for controlling cellular processes. *Acc Chem Res*. 2021;54:2916–2927. doi:10.1021/acs.Aounts.1c00215
125. Beddoes CM, Case CP, Briscoe WH. Understanding nanoparticle cellular entry: a physicochemical perspective. *Adv Colloid Interface Sci*. 2015;218:48–68. doi:10.1016/j.cis.2015.01.007
126. Shen Z, Ye H, Yi X, Li Y. Membrane wrapping efficiency of elastic nanoparticles during endocytosis: size and shape matter. *ACS Nano*. 2018;13:215–228. doi:10.1021/acsnano.8b05340
127. Wang X, Wang Y, He H, et al. Steering graphene quantum dots in living cells: lighting up the nucleolus. *J Mater Chem B*. 2016;4:779–784. doi:10.1039/c5tb02474a
128. Han G, Zhao J, Zhang R, et al. Membrane-penetrating carbon quantum dots for imaging nucleic acid structures in live organisms. *Angew Chem Int Ed Engl*. 2019;58:7087–7091. doi:10.1002/anie.201903005
129. Hua XW, Bao YW, Wu FG. Fluorescent carbon quantum dots with intrinsic nucleolus-targeting capability for nucleolus imaging and enhanced cytosolic and nuclear drug delivery. *ACS Appl Mater Interfaces*. 2018;10:10664–10677. doi:10.1021/acsami.7b19549
130. Su YL, Yu T, Chiang W, et al. Hierarchically targeted and penetrated delivery of drugs to tumors by size-changeable graphene quantum dot nanoaircrafts for photolytic therapy. *Adv Funct Mater*. 2017;27:1700056. doi:10.1002/ADFM.201700056
131. Hui Y, Yi X, Hou F, et al. Role of nanoparticle mechanical properties in cancer drug delivery. *ACS Nano*. 2019;13:7410–7424. doi:10.1021/acsnano.9b03924
132. Cola W, Liu Y, Han R, Bai Q, Hang C. Nano–cell interactions of non-cationic bionanomaterials. *Acc Chem Res*. 2019;52:1519–1530. doi:10.1021/acs.accounts.9b00103
133. Li Q, Fan J, Mu H, Chen L, Yang Y, Yu S. Nucleus-targeting orange-emissive carbon dots delivery adriamycin for enhanced anti-liver cancer therapy. *Chinese Chem Lett*. 2023;35:108947. doi:10.1016/j.cclet.2023.108947
134. Saisyo A, Nakamura H, Fang J, et al. pH-sensitive polymeric cisplatin-ion complex with styrene-maleic acid copolymer exhibits tumor-selective drug delivery and antitumor activity as a result of the enhanced permeability and retention effect. *Colloids Surf B Biointerfaces*. 2016;138:128–137. doi:10.1016/j.colsurfb.2015.11.032
135. Fu X, Shi Y, Qi T, et al. Precise design strategies of nanomedicine for improving cancer therapeutic efficacy using subcellular targeting. *Signal Transduct Target Ther*. 2020;5. doi:10.1038/s41392-020-00342-0
136. Liu J-N, Bu W, Pan L-M. Simultaneous nuclear imaging and intranuclear drug delivery by nuclear-targeted multifunctional upconversion nanoprobes. *Biomaterials*. 2012;33:7282–7290. doi:10.1016/j.biomaterials.2012.06.035
137. Song Y, Li X, Cong S, Zhao H, Tan M. Nuclear-targeted of TAT peptide-conjugated carbon dots for both one-and two-photon fluorescence imaging. *Colloids Surf B Biointerfaces*. 2019;180:449–456. doi:10.1016/j.colsurfb.2019.05.015
138. Yang L, Jiang W, Qiu L, et al. One pot synthesis of highly luminescent polyethylene glycol anchored carbon dots functionalized with a nuclear localization signal peptide for cell nucleus imaging. *Nanoscale*. 2015;7:6104–6113. doi:10.1039/c5nr01080b
139. Yin X, Sun Y, Yang R, Qu L, Li Z. RNA-responsive fluorescent carbon dots for fast and wash-free nucleolus imaging, Spectrochim. *Acta A Mol Biomol Spectrosc*. 2020;237:118381. doi:10.1016/j.saa.2020.118381
140. Hua X-W, Bao Y-W, Zeng J, Wu F-G. Nucleolus-targeted red emissive carbon dots with polarity-sensitive and excitation-independent fluorescence emission: high-resolution cell imaging and in vivo tracking. *ACS Appl Mater Interfaces*. 2019;11:32647–32658. doi:10.1021/acsami.9b09590
141. Zhang Y, Zhang X, Shi Y, Sun C, Zhou N, Wen H. The synthesis and functional study of multicolor nitrogen-doped carbon dots for live cell nuclear imaging. *Molecules*. 2020;25:306. doi:10.3390/molecules25020306
142. Liu H, Yang J, Li Z, et al. Hydrogen-bond-induced emission of carbon dots for wash-free nucleus imaging. *Analy Chem*. 2019;91:9259–9265. doi:10.1021/acs.analchem.9b02147
143. Stępiński D. The nucleolus, an ally, and an enemy of cancer cells, Histochem. *Cell Biol*. 2018;150:607–629. doi:10.1007/s00418-018-1706-5
144. Yang XZ, Du XJ, Liu Y, et al. Rational design of polyion complex nanoparticles to overcome cisplatin resistance in cancer therapy. *Adv Mater*. 2013;26:931–936. doi:10.1002/adma.201303360
145. Peng H, Tang J, Zheng R, et al. Nuclear-targeted multifunctional magnetic nanoparticles for photothermal therapy. *Adv Healthc Mater*. 2017;6. doi:10.1002/adhm.201601289
146. Schirone L, D'Ambrosio L, Forte M, et al. Mitochondria and doxorubicin-induced cardiomyopathy: a complex interplay. *Cells*. 2022;11:2000. doi:10.3390/cells11132000
147. Biswas R, Yang S, Crichton RA, et al. C60-β-cyclodextrin conjugates for enhanced nucleus delivery of doxorubicin. *Nanoscale*. 2022;14:4456–4462. doi:10.1039/D2NR00777K
148. Das M, Singh RP, Datir SR, Jain S. Intranuclear drug delivery and effective in vivo cancer therapy via estradiol–peg-appended multiwalled carbon nanotubes. *Mol Pharm*. 2013;10:3404–3416. doi:10.1021/mp4002409
149. Zheng XT, Ma XQ, Li CM. Highly efficient nuclear delivery of anti-cancer drugs using a bio-functionalized reduced graphene oxide. *J Colloid Interf Sci*. 2016;467:35–42. doi:10.1016/j.jcis.2015.12.052
150. Su W, Guo R, Yuan F, et al. Red-emissive carbon quantum dots for nuclear drug delivery in cancer stem cells. *J Phys Chem Lett*. 2020;11:1357–1363. doi:10.1021/acs.jpclett.9b03891
151. Liu S, Wang J, Li H, et al. Nucleus-targeting carbon quantum dots assembled with gambogic acid via π–π stacking for cancer therapy. *Adv Ther*. 2022;6. doi:10.1002/adtp.202200201

152. Chen Y, Gao Y, Chen Y, Liu L, Mo A, Peng Q. Nanomaterials-based photothermal therapy and its potentials in antibacterial treatment. *J Control Release*. 2020;328:251–262. doi:10.1016/j.jconrel.2020.08.055
153. Gao G, Jiang Y, Jia H, et al. From perinuclear to intranuclear localization: a cell-penetrating peptide modification strategy to modulate cancer cell migration under mild laser irradiation and improve photothermal therapeutic performance. *Biomaterials*. 2019;223:119443. doi:10.1016/j.biomaterials.2019.119443
154. Hua XW, Bao YW, Zeng J, Wu FG. Ultrasmall all-in-one nanodots formed via carbon dot-mediated and albumin-based synthesis: multimodal imaging-guided and mild laser-enhanced cancer therapy. *ACS Appl Mater Interfaces*. 2018;10:42077–42087. doi:10.1021/acsami.8b16065
155. Dou Q, Fang X, Jiang S, Chee PL, Lee T-C, Loh XJ. Multi-functional fluorescent carbon dots with antibacterial and gene delivery properties. *Loh RSC Adv*. 2015;5:46817–46822. doi:10.1039/c5ra07968c
156. Wang P, Zhang L, Zheng W, et al. Thermo-triggered release of CRISPR-Cas9 system by lipid-encapsulated gold nanoparticles for tumor therapy. *Angew Chem Int Ed Engl*. 2018;57:1491–1496. doi:10.1002/anie.201708689
157. Ma H, Tu L-C, Naseri A, et al. CRISPR-Cas9 nuclear dynamics and target recognition in living cells. *J Cell Biol*. 2016;214:529–537. doi:10.1083/jcb.201604115
158. Zhai LM, Zhao Y, Xiao RL, et al. Nuclear-targeted carbon quantum dot mediated CRISPR/Cas9 delivery for fluorescence visualization and efficient editing. *Nanoscale*. 2022;14:14645–14660. doi:10.1039/d2nr04281a
159. Xie R, Lian S, Peng H, et al. Mitochondria and nuclei dual-targeted hollow carbon nanospheres for cancer chemophotodynamic synergistic therapy. *Mol Pharm*. 2019;16:2235–2248. doi:10.1021/acs.molpharmaceut.9b00259
160. Chen HS, Wang Z, Zong S, et al. A graphene quantum dot-based FRET system for nuclear-targeted and real-time monitoring of drug delivery. *Nanoscale*. 2015;7:15477–15486. doi:10.1039/c5nr03454j